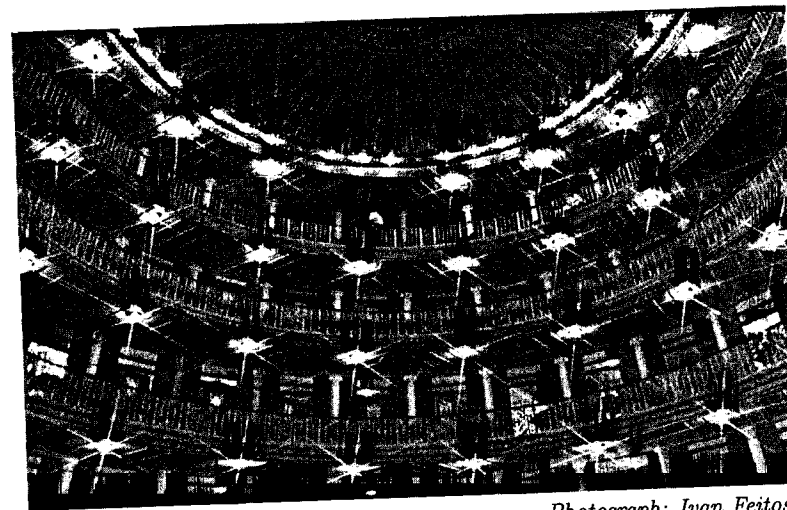


References

- [1] Richard Feynman, *QED*. Princeton University Press, Princeton, NJ, 1985, p. 39.
- [2] H. Jeffreys, On certain approximate solutions of linear differential equations of the second order. *Proc. London Math. Soc.*, 23(1924), pp. 428-436.
- [3] V. G. Boltyanskii, *Mathematical Methods of Optimal Control*. Holt, Rinehart and Winston, New York, 1971.

*Photograph: Ivan Feitosa***Momentum Maps and Geometric Phases***Jair Koiller (coordinator)*

LABORATÓRIO NACIONAL DE COMPUTAÇÃO CIENTÍFICA

AV. GETÚLIO VARGAS 333

PETRÓPOLIS RJ 25651-070, BRAZIL

e-mail: jair@lncc.br

with collaborators

*Earnest W. Coli (Planet Earth)**Richard Montgomery (U.C., Santa Cruz)**Joaquin Delgado Fernandez (UAM, Iztapalapa, Mexico)**Kurt Ehlers (TMCC, Nevada)**Teresinha J. Stüchi (UFRJ, Brazil)**Maria de Fátima L. B. P. Almeida (UERJ, Brazil)*

Foreword

Momentum maps are one of the cornerstones of geometric mechanics. In these lectures, we present three related situations in which they are instrumental, summarized in Part 1 (an overview). In Part 2, we study adiabatic phases for integrable mechanical systems in a (slowly) moving frame. *The momentum map of the group is averaged over the invariant tori.* The simplest examples are Foucault's pendulum or any system with S^1 symmetry. A nontrivial example is the rotating elliptic billiard. In Part 3, we give an example of nonadiabatic phases, extending work by Montgomery and Levi on Euler's rigid body motion. We find the geometric phase around the angular momentum vector of a *gyrostat*. Here the momentum acts as a "pillar" around which the geometric phases are depicted. In Part 4, we make the restriction of zero momentum. Typically, the configuration space is a principal bundle with a connection; the base is called the "shape space." *A robot (or an organism) can control its shape and by so doing can navigate in the configuration space.* After one cycle of shape deformations, the new position differs from the original by an element of the Lie group. We assume the reader has had an undergraduate-level analytic mechanics class and knows the basic facts about symplectic forms, canonical transformations, and momentum maps of groups acting symplectically. Part 4 requires knowledge of principal bundles and connections (actually, it can be used to motivate that theory).

Our work, a companion to sections 2 and 3 of Mark Levi's lectures (Chapter 7 of this volume), is based on a set of four lectures given in January 1999 at the Mathematics Department, Universidade Federal de Pernambuco, Brazil. I would like to thank Hildeberto Cabral for his friendship and support for almost 35 years!

Misrepresentations are the coordinator's responsibility. To excuse ourselves, we quote Mark Twain: "Adults don't really lie, they just exaggerate" (*Tom Sawyer*) and Oscar Wilde "It is a terrible thing for a man to find out suddenly that all his life he has been speaking nothing but the truth." (*The importance of being Earnest.*)

Earnest W. Coli is an intelligent *Escherichia coli* which is the mascot for our collective work. See the site: <http://web.bham.ac.uk/bcm4ght6/res.html>, the E. Coli homepage.

The collaboration of the participants is as follows:

- Part 2: Classical Adiabatic Angles
With Richard Montgomery, Mathematics Department, University of California, Santa Cruz 95064, USA.
- Part 3: Holonomy for Gyrostats
With Maria de Fatima L. B. de Paiva Almeida, PUC-RJ, and Teresinha J. Stuchi, Instituto de Física da UFRJ, Brazil.
- Part 4: Microswimming
With Kurt M. Ehlers, Truckee Meadows Community College, Reno, Nevada 89512, USA, and Joaquin Delgado Fernandez, UNAM-Iztapalapa, Mexico.

Part 1: Overview

1 Adiabatic Phases: Overview

Berry [4] and Hannay [10] showed, around 1985, that geometrical and topological effects are ubiquitous in classical and quantum mechanical systems subject to *adiabatic* variations of parameters. Since then, the theme “geometric phases in physics” has exploded¹.

Our examples in Part 2 will fit in the following framework². Consider a configuration space S of dimension n and a natural mechanical system on TS with Lagrangian $L = T - V$. S (the “laboratory”) is immersed on a bigger Riemannian manifold W (the “universe”) of dimension N . W is acted upon by a Lie group G so that every map $i_g : S \rightarrow g \cdot S$ is an isometry. Using the metric, we have the identifications $TS \cong T^*S$, $TW \cong T^*W$, and the embedding $TS \rightarrow TW$ yields the corresponding *symplectic embedding* $T^*S \rightarrow T^*W$ (not to be confused with the *projection* $T^*W \rightarrow T^*S$ corresponding to the dual of $TS \hookrightarrow TW$).

Given a curve $t \rightarrow g(t) \in G$,

$$L(Q, \dot{Q}, t) = T\left(\frac{d}{dt}(g(t)Q)\right) - V(Q), \quad Q \in S, \quad (1)$$

is a moving Lagrangian system inside W . As is well known, Euler–Lagrange equations for the generalized coordinates Q contain “fictitious” forces, such as Coriolis and centripetal ([2, chapter 4]). It is more convenient for our purposes to work directly in the underlying inertial frame W . We set

$$q(Q, t) = g(t)Q \quad (2)$$

so the Lagrangian (1) becomes³

$$L(q, \dot{q}, t) = T(\dot{q}) - V(g(t)^{-1} \cdot q). \quad (3)$$

The Lie group G can be thought of as a parameter space.

¹For a comprehensive introduction, see [24].

²See [12] for a souped up version of the theory.

³One of the nicest features of the formalism of calculus of variations is the invariance of Euler–Lagrange equations [2, section 12D]. Lagrangian (3), in which the time-dependence is transferred to the potential energy, is *mathematically* equivalent to Lagrangian (1) through the coordinate change (2). Notice that (3) can also represent a *physically* distinct problem.

The potential V contains three types of terms:

$$V = V_{s.c.} + V_{int} + V_{ext}.$$

$V_{s.c.}$ are *infinitely constraining* potentials (see, e.g., [23] or [13]) to S . This means that $g(t)^{-1}q \in S$ throughout the motion. Terms in V that are completely equivariant under G , $V_{int}(g^{-1} \cdot q) = V_{int}(q)$ form the *internal* or *interaction* potential. The remaining terms define the *external* potential.

Given a slow variation $g = g(et)$, $g(0) = I$ describing a closed curve $C \subset G$, we want to compare the moving system (1) with a system evolving in the inertial frame ($g \equiv I$).

As a basic example, we consider a spherical pendulum orbiting a planet⁴. To simplify matters, we assume that our spaceship is the spherical pendulum itself. Taking the origin at the planet, the center of the sphere describes a curve $r(t) \in W = \mathbb{R}^3$. In the inertial frame W we have

$$H(p, q, t) = \frac{1}{2} |p|^2 - \frac{k}{|q|} + \mu(|q - r(t)| - 1)^2, \quad \mu \rightarrow \infty, \quad (4)$$

where k is the planet’s attraction constant and units are such that the length of the rod and the mass of the particle are 1. The usual Foucault pendulum corresponds to $r(t)$, describing a parallel (constant latitude circle) of the planet. See Figure 1.

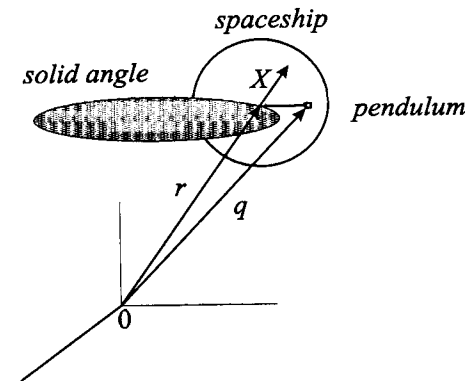


Figure 1. The “Star Wars” Foucault pendulum. Holonomy is given by a solid angle.

⁴This is a “Star Wars” Foucault pendulum.

We do not need to linearize gravity, nor to require that the pendulum is in the small oscillation regime. We just use the S^1 symmetry around the axis

$$x = \frac{r(t)}{|r(t)|}.$$

We consider any moving frame $R(t) \in SO(3)$ whose third axis is $x(t) = r(t)/|r(t)| \in S^2$. Here the change of coordinates (2) is

$$q = r + R(x)Q, \quad r = |r| \cdot x, \quad R(x)e_3 = x = r/|r|. \quad (5)$$

Given any integrable system with S^1 symmetry around e_3 , we use the angle θ around this axis as one of the generalized coordinates⁵. We do not care about the remaining generalized coordinates, because there will be no effect on them to first order on ϵ . Let the system evolve in an inertial frame ($r(t) \equiv r_o$); the function

$$\theta = \theta_{dyn}(t) \quad (6)$$

is called the *dynamic phase*.

Now, let the spaceship go, as it actually does; notice that $r = r(\epsilon t)$ is slow compared to the frequencies of the system. We will show that when the spaceship makes a complete cycle, coordinate θ will have acquired an extra *geometric phase* (of order $1 = \epsilon^0$) given by

$$\Delta\theta_{\text{geometric}} = \text{solid angle subtended by } r(t). \quad (7)$$

Note that the parameter space $G = SE(3)$ reduces here to $X = \mathbb{R}^3 - 0 \equiv S^2 \times \mathbb{R}^*$. The curve $r(t)$ of the pendulum pivot can be retracted to its S^2 projection x , and the geometric phase is precisely the spherical angle. See Figure 1 again.

The dynamic phase is of order ϵ^{-1} , so the geometric phase usually can only be extracted⁶ by interference with a twin system evolving in the inertial frame.

⁵Caveat: This does not necessarily imply that θ must be one of the uniformizing (i.e., part of an action-angle coordinate system) coordinates. In fact, for the spherical pendulum θ is not an angle coordinate.

⁶In Foucault's pendulum, which swings vertically, the dynamic phase vanishes identically, so the geometric phase effect can be seen directly!

2 Nonadiabatic Phases of Gyrostats

Recall Euler's rigid body motion with a fixed point. With the help of Lie groups, one can describe the motion as follows. The configuration space is the group $SO(3)$ of orthogonal matrices. Rigid body motions $R = R(t)$ are *geodesics* of a *left-invariant Riemannian metric* on $SO(3)$, since the Lagrangian consists of kinetic energy alone⁷.

Due to Noether's theorem, it follows that the angular momentum (written on the inertial frame coordinates) is a conserved vector,

$$m(t) \equiv m. \quad (8)$$

Euler's reduced equations⁸ describe the motion $M(t)$ of the angular mo-

Momentum sphere $|M| = J$

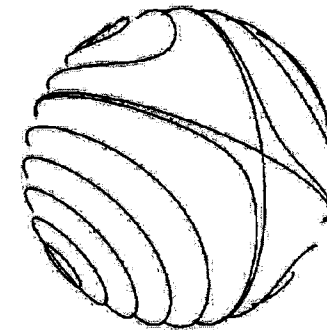


Figure 2. Euler's reduced system for the phase curves $M(t)$.

mentum m as viewed from the rotating body. Following Arnold's notation [2], every capital vector means an object written in the body frame:

$$R(t)M(t) = m.$$

⁷*Left-invariance* is the mathematical wording of the fact that physical behavior does not depend on the choice of coordinate axis x, y, z for the inertial frame.

⁸*Reduction* goes back to Jacobi's "elimination of a node" and was cast in modern language by Marsden and Weinstein [17]. If the reduced system is integrable, the problem of finding the time-dependence of the "ignorable" coordinates was often dismissed on the argument that it can be done easily by quadratures. But the reconstruction is not always easy. A bit of geometry can be of great help, especially when the symmetry group is nonabelian. For a general theory for *reconstruction* of the complete solutions of Hamiltonian systems with group symmetry, see [18].

Differentiating, after some simple manipulations, one gets

$$\frac{d\mathbf{M}}{dt} = \mathbf{M} \times \nabla_{\mathbf{M}} H(\mathbf{M}) \quad (9)$$

with $H(\mathbf{M}) = \frac{1}{2}(\mathbf{M}, \mathbf{A}^{-1}\mathbf{M})$. The inertia matrix \mathbf{A} is symmetric and positive definite. The reduced phase portrait on the sphere $\|\mathbf{M}\| = J$ is sketched in Figure 2.

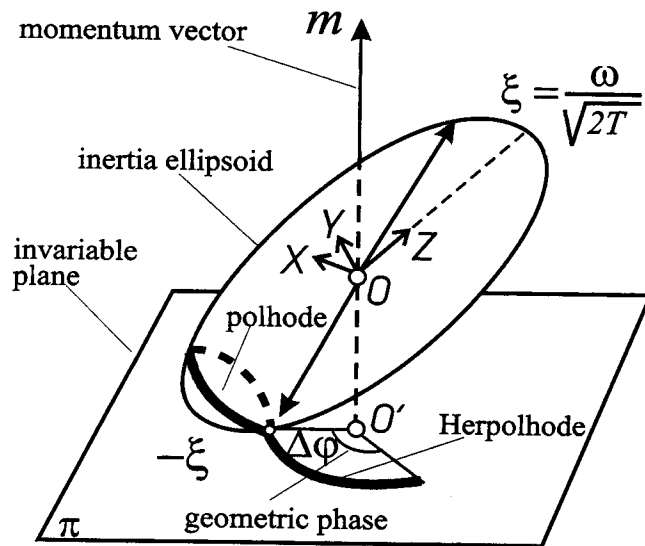


Figure 3. Poincaré's description of the rigid body motion. The geometric phase is $\Delta\phi$.

Reconstruction can be geometrically visualized in Poincaré's description: the inertia ellipsoid (carrying the body frame $R(t) : XYZ$) rolls without slipping over the invariable plane [2]. Figure 3 depicts a *polhode* in the ellipsoid and the corresponding *herpolhode*.

Recall that $R \in SO(3)$ is parametrized by the three Euler angles (see Figure 4)

$$\varphi = \angle(x, \text{nodes}), \quad \psi = \angle(\text{nodes}, X), \quad \sigma = \angle(Z, z). \quad (10)$$

What is the geometric phase $\Delta\phi$ around $\bar{\mathbf{m}}$?

Using a bit of symplectic abstract nonsense, Montgomery [19] found

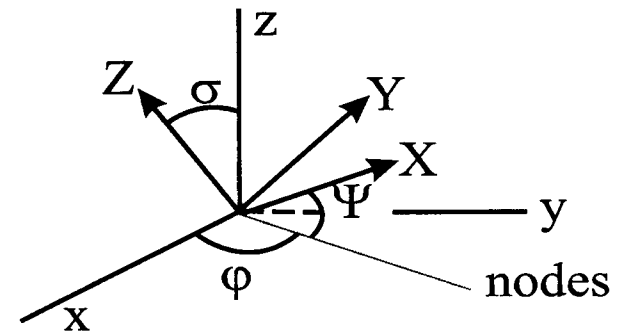


Figure 4. Euler angles. $\bar{\mathbf{m}}$ along the z -axis. Holonomy is measured using ϕ .

the following formula⁹:

$$\Delta\phi = \frac{2hT}{J} - \Upsilon. \quad (11)$$

Here h is the energy of the trajectory, J is the modulus of the angular momentum vector, T is the period of the polhode, and Υ is the (signed) solid angle, swept by the polhode. This solid angle is also the (normalized, signed) area enclosed by the curve $\mathbf{M}(t)$ in Euler's phase portrait!

Thus, we do not need elliptic functions to get the most important information about the full rigid body motion. The herpolhode angular shift is given directly in terms of the reduced Euler system (the polhode spherical angle).

More generally, take any system with symmetry and consider a *periodic* solution of the reduced system. Reconstructing the full solution, some variables usually acquire *holonomies*. In many cases, differential geometric insight allows one to split a phase into two parts, one of which is called "dynamic phase," as is the first term on the right-hand side of (11), while the other is called "geometric phase," as is the solid angle in (11).

Here we will extend (11) to *gyrostats*, mechanical systems that are composed of more than one body yet have the rigid body property that its inertia components are time independent constants [25, 16]. Such systems consist of a main rigid body, called the *carrier*, together with one or more

⁹Also obtained by M. Levi using differential geometry (see Levi's chapter 7 in this book).

rigid symmetric rotors, which we may call *flywheels*, supported by rigid bearings on the carrier. See Figure 5. Gyrostats have important technological applications, particularly in the attitude control of artificial satellites [15, 11]. Rotations of the n flywheels relative to the carrier do not change

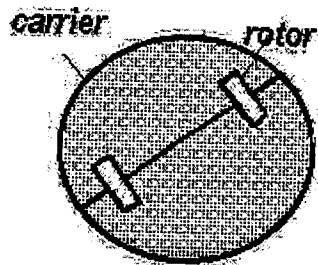


Figure 5. A gyrostat with one rotor or flywheel.

the mass geometry of the whole system. For a gyrostat with n flywheels, the configuration space is $SO(3) \times S^1 \times \dots \times S^1$. We denote the additional degrees of freedom $\theta_1, \dots, \theta_n$. In addition to *left (or spatial)* $SO(3)$ invariance, there is also *right (or material)* $S^1 \times \dots \times S^1$ symmetry. In this case Noether's theorem implies the existence of n additional conserved scalar momenta I_1, \dots, I_n , besides the conserved vector \mathbf{m} .

The reduced equations of motion also give rise to trajectories on the sphere $\|\mathbf{M}\| = J$. They are given by

$$\frac{d\mathbf{M}}{dt} = \mathbf{M} \times \nabla_{\mathbf{M}} H(\mathbf{M}, I), \quad \frac{d\theta}{dt} = \nabla_I H(\mathbf{M}, I). \quad (12)$$

The reduced Hamiltonian $H(\mathbf{M}, I)$ is given by a quadratic function of $3+n$ variables $M_1, M_2, M_3, I_1, \dots, I_n$. In the first set of equations, the conserved momenta I_1, \dots, I_n are thought of as parameters. We have shortened the notations, $\theta = (\theta_1, \dots, \theta_n)$ and $I = (I_1, \dots, I_n)$ for the flywheel coordinates and momenta. Once a closed trajectory $C : \mathbf{M} = \mathbf{M}(t)$ is found, say with period T , the phases associated to the flywheels can be found by quadratures:

$$\Delta\theta_j = \int_0^T \nabla_{I_j} H(\mathbf{M}(t), I) dt. \quad (13)$$

What about the geometric phase $\Delta\phi$ of the main body? Using Montgomery's approach, we prove

$$\Delta\phi = \frac{2hT}{J} - \gamma - \frac{1}{J} \sum_{j=1}^n I_j \Delta\theta_j. \quad (14)$$

We obtained the same result following Levi's method; see [1].

3 Holonomy with Zero Momentum

In this section we present the abstract framework in a nutshell¹⁰. The reader not acquainted with connections on principal bundles should read Part 4 first.

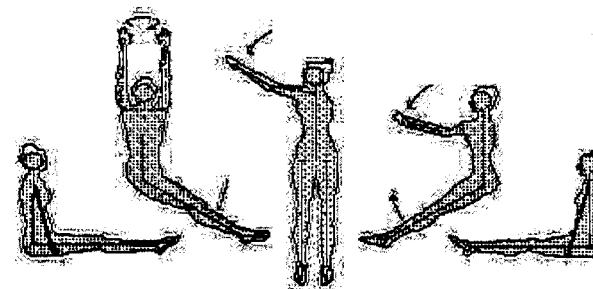


Figure 6. A cat performing holonomy (adapted from [9]).

The configuration space Q for self-locomotion problems¹¹ is a principal bundle $\pi : Q \rightarrow S$ over a base manifold S , with group G . That is, G acts on Q and $S = Q/G$ is the space of "shapes." Q has a G -invariant Riemannian metric, inherited by S . Denote $V_q = T_q\pi^{-1}(s)$ the vertical distribution. The statement

$$H = V^\perp \quad (\text{with respect to the metric}) \quad (15)$$

defines a *mechanical connection*.

We assume that this connection is *fat* (has lots of curvature). By the Ambrose and Singer theorem [7, p.389], there are admissible paths between any two points $q_0, q_1 \in Q$. Take them in the same fiber, $q_1 = g \cdot q_0$.

¹⁰See [20] for details.

¹¹Examples include the connections for falling cats or gymnasts, deforming molecules, satellites with moving panels, swimming in a tar pool, and many more (Figure 6).

For low Reynolds number swimming, \mathcal{Q} , the set of "located shapes," is the set of embeddings of a given manifold (say, the sphere) on \mathbb{R}^3 . S , the set of "unlocated shapes," is the quotient of \mathcal{Q} by the group $G = SE(3)$ of euclidean motions. An infinitesimal deformation of a given shape in \mathcal{Q} gives a vector field along the shape, and the set of infinitesimal deformations defines the tangent bundle $T\mathcal{Q}$. In Part 4 we show how the connection can be computed.

If a group G acts on a manifold Q and \langle, \rangle is a G -invariant Riemannian metric, recall that the momentum map $\mu: TQ \rightarrow \mathcal{G}^*$ is given by

$$\mu(v_q) \cdot \xi = \langle \xi_q, v_q \rangle, \quad \xi_q = \left. \frac{d \exp(t\xi)}{dt} \right|_{t=0} \cdot q, \quad \xi \in \mathcal{G}, v_q \in T_q Q, \quad (16)$$

where we have identified $TQ \cong T^*Q$ via the metric.

There is an intrinsic formulation for the connection form. Define the *locked inertia tensor*, $I: \mathcal{G} \rightarrow \mathcal{G}^*$, by

$$I_q(\xi) \cdot \eta = \langle \xi_q, \eta_q \rangle. \quad (17)$$

The connection form is

$$A(v_q) = I_q^{-1}(\mu(v_q)). \quad (18)$$

The horizontal distribution is the kernel of the momentum map¹² μ .

For a cycle $s(t)$ of infinitesimal deformations of a shape s spanned by vectors $\epsilon u_1, \epsilon u_2, -\epsilon u_1, -\epsilon u_2 x \in T_s$, the holonomy is given by

$$g \sim \exp(\epsilon^2 \Omega(u_1, u_2)),$$

where Ω is the curvature of the connection.

Problem. With prescribed holonomy $g \in G$, find the shortest loop $s(t)$ in S such that its horizontal lift connects q_0 to $q_1 = gq_0$. The elements $\dot{s} \in TS$ are viewed as *controls*.

This variational problem with constraints is a special *sub-Riemannian* geometry problem. Montgomery [20] studied the beautiful structure of the corresponding Euler-Lagrange equations, given by

$$\frac{ds_j}{dt} = p_j, \quad \frac{dp_j}{dt} = -\frac{1}{2} \frac{\partial g^{ik}}{\partial x_j} p_i p_k + F_{jk}^I p^k \xi_I, \quad \frac{d\xi_I}{dt} = -c_{IJ}^K A_j^J p^j \xi_K, \quad (19)$$

¹²In the case of microswimming, zero momentum means that the organism can exert neither net force nor torque on the fluid.

where A_j^J and F_{jk}^I are, respectively, the coefficients of the connection and the curvature forms. Here j runs over the dimension of S and I over the dimension of the group. The intrinsic formulation of these equations, known in the Yang-Mills theories as Wong's equations, are

$$\langle \nabla_{\dot{\gamma}} \dot{\gamma}, \bullet \rangle = \lambda \cdot F(h\dot{\gamma}, h\bullet), \quad \frac{D\lambda}{dt} = 0, \quad (20)$$

where $\lambda(t)$, the Lagrange multiplier, belongs to $Ad^*Q = Q \times_{Ad} \mathcal{G}^*$, an associated fiber bundle over S with fiber \mathcal{G}^* . Here h denotes the horizontal lift via the connection. There is an Ad-ambiguity in the value of F , choosing different elements $q \in Q$ over the vertical fiber over $s \in S$. This ambiguity is cancelled with the corresponding Ad*-ambiguity of λ . The optimal trajectories in the total space Q are obtained from the projections $s(t) \in S$ by horizontal lift.

Not developed further in these notes due to space limitations, we briefly discuss *nonholonomic systems*, a theme regarded until a few years ago as only curious or bizarre, but that has recently become of great interest in robotics¹³. One example is certain stones, known to the Celts and supposedly possessing magical properties, that prefer to rotate in one direction (experiment performed in class). This and other examples show that the momentum map is often *not conserved* in nonholonomic systems!

For nonholonomic mechanical systems such as those encountered in engineering applications, using d'Alembert's principle is believed to be the correct way to eliminate the constraints (Sommerfeld [22])¹⁴.

In the case of nonholonomic systems with symmetry, eliminating the constraints leads to an interesting reduced system (for details, we refer to our work [14]). In the simplest situation, the same ingredients are used: a principal bundle Q over a base manifold S , with group G , a G -invariant Riemannian metric (or more generally, a G -equivariant Lagrangian L on Q), and finally a connection, whose horizontal spaces define the constraints. Here, however, the horizontal spaces do not need to be orthogonal to the

¹³Notwithstanding a somewhat dubious reputation, nonholonomic systems attracted the interest of important scientists in the past. Hertz advocated replacing forces by constraints and Cartan made an interesting address at the 1928 IMU Congress [6]. See [8] for the state of the art of nonholonomic systems.

¹⁴As Hertz already knew, a different set of equations results if one uses the rules of calculus of variations (as in (20)). But their solutions do not fit the results of experiments. Paraphrasing Leibniz, the engineer's world is not the best (nor the worst), so it is not described by variational principles.

vertical spaces.

Using the horizontal distribution, the equivariant Lagrangian L on TQ projects to a Lagrangian L^* on TS , but with an extra "strange" force!

We denote (following Arnold [3]) by $[L^*](v_s) \in T_s^*S$ the Euler-Lagrange derivative¹⁵. The reduced equations of motion on T^*S are written as (see [14])

$$[L^*](v_s)(\bullet) = \mu(\text{FL}h_q(v_s)) \cdot \Omega(h_q(v_s), h_q(\bullet)). \quad (21)$$

Here $q \in Q$ is any point on the fiber over s , h_q is the horizontal lift operator, FL is the Legendre transform associated to L , $\text{FL} : TQ \rightarrow T^*Q$, and Ω is the curvature of the connection. Figure 6 exemplifies reorientation manouvers performed by cats, gymnasts, and astronauts (without violating the constraint of total zero angular momentum). Not surprisingly, the momentum map μ is the key ingredient in this strange force.

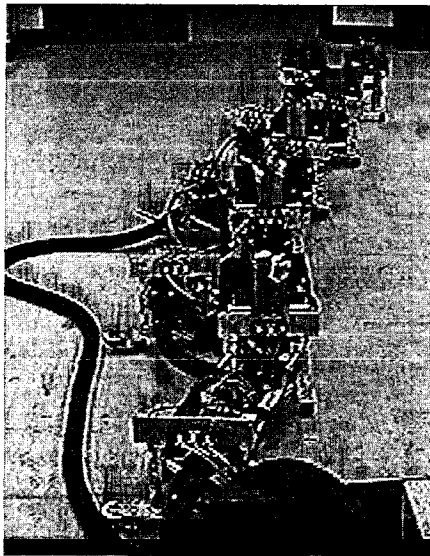


Figure 7. Snakeboard (from [5], with permission from the authors). Shape variables: (ψ, ϕ_1, ϕ_2) . Lie group variables (x, y, θ) .

Once the reduced equations are solved, the full motion is recovered on Q by horizontally lifting the trajectory $s(t)$.

¹⁵In coordinates, the familiar $\frac{d}{dt} \left(\frac{\partial L^*}{\partial \dot{s}_i} \right) - \frac{\partial L^*}{\partial s_i}$, which transforms as a covector.

To finish, we would like to mention a hybrid situation, in which the nonholonomic system depends on parameters that can be used as control variables. This new feature, which allows potential applications in robotics, especially in biomechanics, was first studied by Jerry Marsden and his associates; see [5]. A delightful example is the snakeboard, (see Figure 7) which is a souped-up version of a skate. The rider can twist his body (coordinate ψ) and turn the front and back pairs of wheels (coordinates ϕ_1, ϕ_2).

The structure of such *D'Alembert control systems* is as follows: denote g the group variables, μ the momentum, and s the parameters that describe the shape of the system. At a glance, the equations of motion have the form

$$g^{-1}\dot{g} = -A(s)\dot{s} + B(\tau)\mu \quad (\text{geometric phase}), \quad (22)$$

$$\dot{\mu} = \dot{s}^\dagger (\alpha(s)\dot{s} + \beta(s)\mu) + \mu^\dagger \gamma(s)\mu \quad (\text{momentum}), \quad (23)$$

$$M(\tau)\ddot{s} = -C(s, \dot{s}) + N(s, \dot{s}, \mu) + \tau \quad (\text{shape dynamics}). \quad (24)$$

If in (24) the forcing $\tau \equiv 0$, the shape varies solely by the nonholonomic dynamics. The rider can impose a full control over s . Equation (24) is deleted and a prescribed $s(t)$ is imposed in the first two equations. The reader should study Figure 8 and convince himself (herself) that indeed μ (momentum about p) is *not* conserved.

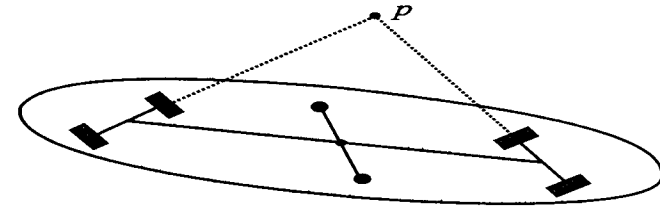


Figure 8. Angular momentum about p is not conserved. Not even p is conserved.

Summarizing: We have described three (four, if we include nonholonomic systems) situations where momentum maps and geometric phases interplay through adiabatic change of parameters, reconstruction, or geometric control. We anticipate that interesting examples will be found in which these features appear simultaneously.

References

- [1] Almeida, M. F. L. B. P., Koiller, J., Stuchi, T. J., *Toy tops, gyrostats and Gauss-Bonnet*, *Matem. Contemp.* **9**, 1–14 (1993).
- [2] Arnold, V., *Méthodes mathématiques de la mécanique classique*, MIR, Moscow (1978).
- [3] Arnold, V. ed., *Dynamical Systems III*, Springer Encyclopaedia of Math. Sciences vol. 3, Springer-Verlag, New York (1988).
- [4] Berry, M. V., *Classical adiabatic angles and quantal adiabatic phase*, *J. Phys. A* **18**, 15–27 (1985).
- [5] Bloch, A. M., Krishnaprasad, P. S., Marsden, J. E., Murray, R. M., *Nonholonomic systems with symmetry*, *Arch. Rational Mech. Anal.* **136**, 21–99 (1996).
- [6] Cartan, E., *Sur la représentation géométrique des systèmes matériels non holonomes*, *Proc. Int. Cong. Math.* vol 4, Bologna, 253–261 (1928).
- [7] Choquet-Bruhat, Y., DeWitt-Morette, C., and Dillard-Bleick, M., *Analysis, manifolds and physics*, North Holland, Amsterdam (1982).
- [8] Cushman, R., Snyaticki, J., eds., *Proc. Workshop on Nonholonomic Constraints in Dynamics, Calgary 1997, Reports on Mathematical Physics*, **42**, 1/2 (1998).
- [9] Frohlich, C., *The physics of somersaulting and twisting*, *Sci. American* **263** 155–164 (1980).
- [10] Hannay, J. H., *Angle variable holonomy in adiabatic excursion of an integrable hamiltonian*, *J. Phys. A* **18**, 221–230 (1985).
- [11] Hubert, C. H., *An attitude acquisition technique for dual-spin spacecraft*, Ph.D. thesis, Cornell University, Ithaca, NY (1980).
- [12] Koiller, J., *Classical adiabatic angles for slowly varying mechanical systems*, *Contemp. Math.* **97**, 159–185 (1989).
- [13] Koiller, J., *A note on classical motions under strong constraints*, *J. Phys. A* **23**, L521–527 (1990).
- [14] Koiller, J., *Reduction of some classical non-holonomic systems with symmetry*, *Arch. Rational Mech. Anal.* **118**, 113–148 (1992).
- [15] Krishnaprasad, P. S., *Lie Poisson structures on dual spin spacecraft and asymptotic stability*, *Nonlinear Anal.* **9:10**, 1011–1035 (1985).
- [16] Leimanis, E., *The General Problem of the Motion of Coupled Rigid Bodies about a Fixed Point*, Springer-Verlag, New York (1965).
- [17] Marsden, J., Weinstein, A., *Reduction of symplectic manifolds with symmetries*, *Rep. Math. Phys.* **5**, 121–130 (1974).
- [18] Marsden, J. E., Montgomery, R., Ratiu, T., *Reduction, symmetry, and phases in mechanics*, *Mem. Amer. Math. Soc.* **88**, 436 (1990).
- [19] Montgomery, R., *How much does the rigid body rotate? A Berry's phase from the 18th century*, *Am. J. Phys.* **59**, 394–398 (1991).
- [20] Montgomery, R., *The isoholonomic problem and some applications*, *Commun. Math. Phys.* **128**, 565–592 (1990).
- [21] Montgomery R., *Optimal control of deformable bodies and its relation to gauge theory*, in T. Ratiu, ed., *The geometry of Hamiltonian systems*, MSRI 1998 Workshop, Springer-Verlag, New York (1991).
- [22] Sommerfeld, A., *Mechanics*, Academic Press, New York (1952).
- [23] Takens, K., *Motion under the influence of a strongly constraining force*, in *Lecture Notes in Math.*, vol. **819**, Springer-Verlag, New York (1979).
- [24] Shapere, A., Wilczek, F., *Geometric Phases in Physics*, World Scientific, Singapore, Teaneck, NJ (1989).
- [25] Wittenburg, J., *Dynamics of Systems of Rigid Bodies*, B.G. Teubner, Stuttgart (1977).

Part 2: Classical Adiabatic Angles

Geometry glitters, Birkhoff used to say, but to find gold one has to dig harder into analysis. So we begin with a disclaimer: we will omit here important issues related to resonance phenomena¹⁶.

4 Averaging Heuristics

This section presents a geometrical derivation of Hannay's classical adiabatic angles. It is a pleasure to acknowledge conversations with R. Montgomery and A. Weinstein; the reader will find their papers [8, 11, 12] very inspiring.

Let $\theta = (\theta_1, \dots, \theta_n)$ denote angle variables in $T^n = S^1 \times \dots \times S^1$ (n times), and $I = (I_1, \dots, I_n)$ the corresponding action variables. Consider a family of canonical transformations, parametrized by $x \in X$:

$$F : (I, \theta, x) \rightarrow (p = p(I, \theta, x), q = q(I, \theta, x)). \tag{25}$$

More abstractly, we may think of a family, parametrized by $x \in X$, of Lagrangian foliations on a symplectic manifold (M^{2n}, ω) :

$$\{\mathcal{L}_x\}_{x \in X}. \tag{26}$$

We consider a family (again parametrized by X) of completely integrable systems $H(p, q; x) = F(I; x)$. Now take $x = x(t)$ and extend phase space and Hamiltonian in the usual way:

$$\mathcal{H}(p, q, E, t) = H(p, q, t) + E, \quad \omega = dp \wedge dq + dE \wedge dt.$$

Here E is a dummy moment associated to a time "coordinate," such that $\dot{H} = -\dot{E} = \partial H / \partial t$ (since \mathcal{H} is constant). In the extended space the map $(E, t, I, \theta) \rightarrow (E, t, p, q)$ is not canonical: the symplectic form pulls back as

$$\omega = dE \wedge dt + dI \wedge d\theta + (I, t)dI \wedge dt + (\theta, t)d\theta \wedge dt. \tag{27}$$

¹⁶See Lochak and Meunier [8], Golin, Knauf, and Marmi [4], and (for time estimates of the adiabatic approximation) Neishtadt [10].

Here, for $u, v = I, \theta$, or t , (u, v) denotes the Lagrange bracket

$$(u, v) = \frac{\partial p}{\partial u} \frac{\partial q}{\partial v} - \frac{\partial p}{\partial v} \frac{\partial q}{\partial u}. \tag{28}$$

Lagrange brackets are not as famous as Poisson brackets, so, to warm up, we propose a simple exercise.

Exercise 4.1 Let (M^{2n}, ω) be a symplectic manifold, and $H : M \rightarrow \mathbb{R}$ be a Hamiltonian. Given any coordinate system $u = (u_1, \dots, u_{2n})$ Hamilton's equation is written as

$$L(\dot{u}_1, \dots, \dot{u}_{2n})^\dagger = (\partial H / \partial u_1, \dots, \partial H / \partial u_{2n})^\dagger,$$

where L is the matrix of Lagrange brackets

$$L_{ij} = (u_i, u_j) = \omega \left(\frac{\partial}{\partial u_i}, \frac{\partial}{\partial u_j} \right).$$

The relationship with Poisson brackets is transparent: $L^{-1} = P$, where

$$P_{ij} = \{u_i, u_j\}.$$

Exercise 4.2 In our case, the matrix of ω with respect to the basis

$$\partial / \partial E, \partial / \partial t, \partial / \partial I, \partial / \partial \theta$$

is $L = J + K$, where

$$J = \begin{bmatrix} 0 & 1 & 0 & 0 \\ -1 & 0 & 0 & 0 \\ 0 & 0 & 0 & 1 \\ 0 & 0 & -1 & 0 \end{bmatrix}, \quad K = \begin{bmatrix} 0 & 0 & 0 & 0 \\ 0 & (t, I) & (t, \theta) & 0 \\ 0 & (I, t) & 0 & 0 \\ 0 & (\theta, t) & 0 & 0 \end{bmatrix}. \tag{29}$$

Proposition 4.1 In the action-angle coordinates, Hamilton's equations for the time-dependent system $H(I, \theta, x(t))$ are given by

$$L \frac{d}{dt} (E, t, I, \theta)^\dagger = \text{grad } \mathcal{F} = (1, F_t, F_I, 0)^\dagger. \tag{30}$$

Exercise 4.3 Let the parameter x vary slowly in time, $x = x(\epsilon t)$, and K be $O(\epsilon)$. Show that $L^{-1} = -J - JKJ + O(\epsilon^2)$.

Proposition 4.2 *If $x = x(\epsilon t)$, then the Hamiltonian vector field*

$$\frac{d}{dt}(E, t, I, \theta) = L^{-1} \text{grad} F$$

is given by

$$\dot{\theta} = \partial F / \partial I + \langle t, I \rangle + O(\epsilon^2), \quad \dot{I} = -\langle t, \theta \rangle + O(\epsilon^2), \quad (31)$$

$$\dot{E} = -\partial F / \partial t + \langle t, \theta \rangle \partial H / \partial I + O(\epsilon^2), \quad (32)$$

where the Lagrange brackets are $O(\epsilon)$.

Notice that the angle coordinates are *fast* (due to the term $\partial H / \partial I$), and all the other terms are $O(\epsilon)$ or higher and therefore *slow*.

Given any function $f(\theta)$ of the angle variables, we denote by $\langle f \rangle$ the average

$$\langle f \rangle = \frac{1}{(2\pi)^n} \int_{T^n} f(\theta) d^n \theta.$$

The "averaging principle," in its outermost heuristical form (see Arnold, [2, chapter 10, section 52], states that it is "reasonable" to replace (31) by the averaged system¹⁷

$$\dot{\theta} = \partial H / \partial I + \langle t, I \rangle, \quad \dot{I} = -\langle t, \theta \rangle. \quad (33)$$

Caveat: It is not easy to transform the word "reasonable" into sound mathematics. See Neishtadt [10].

Definition 4.4 *Family (25) is free if there is a globally defined generating function $S(I, \theta; x)$ such that*

$$pdq - Id\theta = d_{(I, \theta)} S. \quad (34)$$

From now on, we assume all families of Lagrangian foliations to be free. The reason for this hypothesis is as follows.

Lemma 4.5 *If (26) is free, then $\langle t, \theta \rangle = 0$. So in the averaged system (33),*

$$\dot{I} = 0.$$

¹⁷The idea goes back to work of Gauss on celestial mechanics; he proposed replacing a perturbing object by an annulus of same total mass.

Proof. For fixed x the 1-form $pdq - Id\theta$ is locally exact; that is, locally there exists a function $S(I, \theta; x)$ with $pdq - Id\theta = d_{(I, \theta)} S$. In particular,

$$p\partial q / \partial \theta = I + \partial S / \partial \theta.$$

Differentiating with respect to t , we have

$$pq_{\theta t} + p_t q_{\theta} = S_{\theta t}.$$

Now,

$$\langle t, \theta \rangle = p_t q_{\theta} - p_{\theta} q_t = [-p q_t]_{\theta} + p q_{\theta t} + p_t q_{\theta} = [-p q_t + S_t]_{\theta}. \quad (35)$$

Since the average of a $\partial / \partial \theta$ is zero, we are done. ■

We say that I is an *adiabatic invariant*. Heuristically, one expects that the solution $I(t)$ of the full system stays close to $O(\epsilon)$ from the initial value, at least for times of order $O(1/\epsilon)$. However, due to resonances, this is not necessarily true for systems with more than one degree of freedom [10].

Having said that, we will proceed bluntly with the averaged equations,

$$\dot{\theta} = \partial H / \partial I + \langle t, I \rangle, \quad \dot{I} = 0. \quad (36)$$

5 The Classical Adiabatic Phases

Curiously, it was only around 1985 that attention was given, by Hannay and Berry, to the extra term in the equation for $\dot{\theta}$. The solution of the averaged system (36) is given as follows.

Theorem 5.1

$$\theta(T) - \theta(0) = \int_0^T H_I(I, t) dt + \int_C \rho dx, \quad \rho = \langle x, I \rangle dx, \quad (37)$$

where

$$\langle x, I \rangle = \frac{1}{(2\pi)^n} \int_{T^n} (p_x q_I - p_I q_x) d^n \theta. \quad (38)$$

The first term in (37) gathers the *dynamic phases*, while the second term gathers the *geometric phases*. Geometric phases are indeed geometric: their value does not depend on reparametrizations of the curve $C : x =$

$x(\epsilon t) \in X$. They depend solely on the family of Lagrangian foliations, not on the specific time-dependent Hamiltonian.

Definition 5.2 The 1-form ρ in parameter space, depending on I , with values on \mathbb{R}^n , is called the Hannay–Berry 1-form.

Remark 5.3 For those familiar with principal bundles: since ρ has vector values, one suspects that it defines a connection on a torus bundle over X (fixing the values of I). See Montgomery [9]. More generally, can one define a connection for adiabatic variations of general systems, not necessarily integrable? See Weinstein [13].

Exercise 5.4 Prove Berry's original expression

$$\langle x, I \rangle = \text{grad}_I \langle -pq_x + S_x \rangle.$$

Although C can be an open curve, in most cases we are interested in finding the geometric phase for a closed curve C in parameter space. If C bounds a disk inside X , we can use Stokes's theorem.

Theorem 5.5

$$d\rho = -\text{grad}_I \beta. \quad (39)$$

Here β is a real-valued 2-form, given by

$$\beta(I) = \frac{1}{(2\pi)^n} \int_{\theta \in T^n} \sum_{i < j} (x_i, x_j) dx_i \wedge dx_j, \quad (40)$$

and where (x_i, x_j) are the Lagrange-like brackets

$$(x_i, x_j) = \sum_k \left(\frac{\partial p_k}{\partial x_i} \frac{\partial q_k}{\partial x_j} - \frac{\partial p_k}{\partial x_j} \frac{\partial q_k}{\partial x_i} \right). \quad (41)$$

Exercise 5.6 Prove Theorem 5.5.

Hint. Use Exercise 5.4. You can also start directly with (38). When computing $d\rho$, interchange some indices. For instance,

$$\sum p_{I x_i} q_{x_j} dx_i \wedge dx_j = - \sum p_{I x_j} q_{x_i} dx_i \wedge dx_j.$$

Terms like $\sum p_{x_i x_j} q_I dx_i \wedge dx_j$ vanish. Notice the minus sign in (39) and the sum $\sum_{i < j}$ in (40). ■

Definition 5.7 β is called the Hannay–Berry 2-form, a 2-form in parameter space X depending on the value I of action variables.

Exercise 5.8 For fixed values of (I, θ) , define the function

$$\lambda_{(I, \theta)} : X \rightarrow M^{2n}$$

using the family (25). Then

$$\sum_{i < j} (x_i, x_j) dx_i \wedge dx_j = \lambda_{(I, \theta)}^* \omega, \quad (42)$$

where ω is the symplectic form on M .

Given a closed curve C in parameter space, bounding a disk $D \subset X$, denote by $D(I, \theta) \subset M$ the image of D under $\lambda_{(I, \theta)}$:

$$D(I, \theta) = \lambda_{(I, \theta)}(D).$$

Proposition 5.1 The geometric phases can be written in an almost intrinsic way as

$$-\text{grad}_I \left\langle \int_{D(I, \theta)} \omega \right\rangle. \quad (43)$$

Remark 5.9 (i) To make this expression completely intrinsic, one needs to study its dependence on changes of action-angle variables $(I, \theta, x) \rightarrow (J, \phi, x)$. (ii) Weinstein used (42) as a starting point to define new invariants for loops of symplectomorphisms on compact symplectic manifolds [12].

We finish this section with a question: Relax the freeness hypothesis (Definition 4.4) for (26). Is there any new term, of topological origin, present in the classical adiabatic angles?

6 Pendulum with Slowly Varying Gravity

This example is closely related to the Foucault pendulum. Take units so that mass, gravity constant, and length are all equal to 1. We have

$$H(p, q, x) = \frac{1}{2}|p|^2 + (q, x) \quad (44)$$

with $q \in S^2$, $(p, q) = 0$, and $x \in X = S^2$ gives the direction of the force of gravity.

The spherical pendulum is obviously integrable because of the S^1 symmetry. Fix $x = e_3$, the north pole, so the gravity vector is $\vec{g} = -ge_3$. One of the momenta, say I_1 , is the angular momentum about e_3 . The other, I_2 , is the area enclosed by the energy curve in the reduced one-degree-of-freedom system (a complete elliptic integral).

The solutions require elliptic functions (of time). In the case of the simple pendulum, three different sets of action-angle variables are needed, one for the libration regime and the other two (essentially the same) for the circulation regimes. It was recently found that it is impossible to find global action-angle coordinates for the spherical pendulum!¹⁸

Exercise 6.1 Make a bibliographical search and get the solutions of the simple (planar) pendulum and of the spherical pendulum in terms of elliptic functions. In other words, find explicitly the canonical transformations

$$P = P(I, \theta), \quad Q = Q(I, \theta), \quad (45)$$

where Q are the Cartesian coordinates and $P = \dot{Q}$ the corresponding momenta.

For the parametrized system (44), we may write

$$q = R(x)Q(I, \theta), \quad p = R(x)P(I, \theta), \quad (46)$$

where (P, Q) are given by (45) and $R: S^2 \rightarrow SO(3)$ satisfies $R(x) \cdot e_3 = x$; that is, $R(x)$ has x as the third column.

Exercise 6.2 R does not exist globally!

¹⁸There is a *monodromy* phenomenon in any domain $I = (I_1, I_2) \in D$ around the unstable equilibrium. We will not discuss this beautiful issue here; see [3].

Hint. The sphere is not “parallelizable”; even worse, it is not “combable.”

Exercise 6.3 Try the mission impossible of constructing R globally. (i) Consider stereographic projection $T_p S^2 \sim \mathbb{R}^2 \rightarrow S^2 - \{-p\}$, with rays emanating from $-p$. Via the differential, map the Euclidian (parallel) frame on $T_p S^2 \cong \mathbb{R}^2$ to a frame on $S^2 - \{-p\}$. Then apply Gram-Schmidt orthogonalization. Sketch a picture; how does it look near $-p$? (ii) Obtain a more familiar picture mapping the polar coordinates frame on $\mathbb{R}^2 - 0$ to the meridian-parallel frame on $S^2 - \{p, -p\}$. What happens at p and $-p$?

At first sight, performing the averages over the tori in (40) using the action-angle system (45) seems to be a byzantine exercise involving elliptic functions. However, from the special “isotropic” form of the canonical transformation (46), we have the following.

Exercise 6.4

$$\beta = f(I_1, I_2) \quad \text{area element of } S^2. \quad (47)$$

Exercise 6.5 To find $f(I_1, I_2)$, it suffices to compute the Lagrange bracket (x_1, x_2) in (40) at $x_0 = e_3$.

Exercise 6.6 Use stereographic coordinates x_1, x_2 at the tangent plane at e_3 , as in Exercise 6.3 (i). Observe that $R(e_3) = I$ and

$$\partial R / \partial x_1 = e_2 \times \cdot, \quad \partial R / \partial x_2 = -e_1 \times \cdot.$$

Draw a picture. Show that the Jacobian at the origin is 1.

Exercise 6.7 Fill in the blanks below. With spherical coordinates

$$Q = \begin{bmatrix} \sin \alpha \cos \beta \\ \sin \alpha \sin \beta \\ \cos \alpha \end{bmatrix}, \quad \dot{Q} = \begin{bmatrix} \dot{\alpha} \cos \alpha \cos \beta - \dot{\beta} \sin \alpha \sin \beta \\ \dot{\alpha} \cos \alpha \sin \beta + \dot{\beta} \sin \alpha \cos \beta \\ -\dot{\alpha} \sin \alpha \end{bmatrix}, \quad (48)$$

compute

$$\begin{aligned} \partial p / \partial x_1 &= e_2 \times \dot{Q} = \cdots, \\ \partial p / \partial x_2 &= -e_1 \times \dot{Q} = \cdots, \end{aligned}$$

$$\begin{aligned}\partial q/\partial x_1 &= e_2 \times Q = \dots, \\ \partial q/\partial x_2 &= -e_1 \times Q = \dots,\end{aligned}$$

$$\sum_k \frac{\partial p_k}{\partial x_1} \frac{\partial q_k}{\partial x_2} - \frac{\partial p_k}{\partial x_2} \frac{\partial q_k}{\partial x_1} = \dots = -\sin^2 \alpha \dot{\beta}. \quad (49)$$

Miracle! The quantity to be averaged over the tori is precisely minus the angular momentum of the spherical pendulum with respect to the axis $x_o = e_3$.

(Here's a shortcut. For the special parametrized family of the form (46),

$$\sum_k \frac{\partial p_k}{\partial x_1} \frac{\partial q_k}{\partial x_2} - \frac{\partial p_k}{\partial x_2} \frac{\partial q_k}{\partial x_1} = -(e_2 \times p)(e_1 \times q) + (e_1 \times p)(e_2 \times q) = p_1 q_2 - p_2 q_1.$$

The argument works for any integrable system with symmetry S^1 (Hannay's top [5] is the simplest example), and parameter space is $X = S^2$. We get $f = -I_1$ in (47) so

$$\beta = -I \text{ area element of } S^2, \quad (50)$$

where I is the momentum associated with the S^1 symmetry. Taking into account the minus sign in (39), we conclude as follows.

Proposition 6.1 For systems $H(\bullet, x)$ with S^1 symmetry around $x \in X = S^2$, the holonomy is the spherical angle in S^2 enclosed by the tip of the symmetry axis x .

7 Slowly Moving Integrable Mechanical Systems

Recall the framework in section 1. We have a natural mechanical system with Lagrangian $L = T - V$ on TS , where S is immersed on a bigger Riemannian manifold W . W is acted upon by a Lie group G so that every map $i_g : S \rightarrow g \cdot S$ is an isometry.

We set

$$q(Q, t) = g(t)Q, \quad p = g(t)^{-1*}P, \quad (51)$$

so that in the Hamiltonian formalism,

$$H(q, p, t) = T(p) + V(g(t)^{-1} \cdot q). \quad (52)$$

The parameter space X is the Lie group G .

As an example, we presented the "Star Wars" Foucault pendulum. Recall (4). As a warmup, we propose a simple exercise.

Exercise 7.1 The linear approximation for $-k/|q|$ is

$$g(t)(q - r(t)) \cdot \frac{r(t)}{|r(t)|}, \quad g(t) = k/|r(t)|^2.$$

As we mentioned before, we need no linearization, nor do we require that the pendulum is in the small oscillation regime. We just use the S^1 symmetry around the axis $x = \frac{r(t)}{|r(t)|}$. The parameter space reduces to $X = \mathbb{R}^3 - 0 = S^2 \times \mathbb{R}^*$. The canonical transformation (46) is now replaced by

$$q = r + R(x)Q, \quad p = R(x)P, \quad (53)$$

where $r = |r| \cdot x$, $R(x)e_3 = x = r/|r|$.

Exercise 7.2 Show that

$$\beta = -I \text{ element of solid angle.}$$

Hint. Show that the affine part in (53) produces no holonomy.

8 Hannay-Berry's 1-Form for Moving Systems

For concreteness, we suppose that $W = \mathbb{R}^{3N}$, with the familiar metric¹⁹

$$T = \sum_i^N m_i \dot{Q}_i^2$$

¹⁹This is not too restrictive due to Nash's embedding theorem.

on $W = \mathbb{R}^{3N}$. Assume that the mechanical system $H = T + V$ in T^*S is completely integrable: there are action-angle coordinates $(I, \theta) \in \mathbb{R}^n \times T^n$ such that $H(P, Q) = K(I)$ under the canonical immersion of $T^*S \rightarrow T^*W$:

$$Q_j = Q_j(I, \theta), P_j = P_j(I, \theta) = m_j \dot{Q}_j = m_j \frac{\partial Q_j}{\partial \theta} \cdot K_I, \quad j = 1, \dots, N. \quad (54)$$

The parameter space X is the Lie group $SE(3) = SO(3) \times \mathbb{R}^3$ acting diagonally on $W = \mathbb{R}^3 \times \dots \times \mathbb{R}^3$. The parametrized family of canonical transformations is given by

$$p_j = RP_j(I, \theta), \quad q_j = RQ_j(I, \theta) + r, \quad j = 1, \dots, N \quad (55)$$

where $g = (R, r) \in SE(3)$.

Theorem 8.1 *The 1-form ρ on $X = SE(3)$ is left invariant and vanishes in the translation subgroup. For any $v \in SO(3)$,*

$$\rho(v) = \text{grad}_I \langle -M(I, \theta) \rangle \cdot v. \quad (56)$$

Here $M \in \mathbb{R}^3$ is the total angular momentum vector, $\langle \cdot, \cdot \rangle$ is the averaging operator, and we identify $so(3) \cong \mathbb{R}^3$ in the usual way:

$$\begin{bmatrix} 0 & -v_3 + v_2 \\ +v_3 & 0 & -v_1 \\ -v_2 + v_1 & 0 & 0 \end{bmatrix} \leftrightarrow \begin{bmatrix} v_1 \\ v_2 \\ v_3 \end{bmatrix}. \quad (57)$$

Proof. The reader should decompress our shortened notation. Theorem 5.1 gives

$$\rho = \langle p_r q_I - q_r p_I \rangle dr + \langle p_R q_I - q_R p_I \rangle dR.$$

The first Lagrange bracket averages to zero. This is because (55) gives $p_r \equiv 0$, $q_r = \text{identity operator}$, and (54) yields

$$p_I = \frac{\partial}{\partial \theta} (m K_I \cdot Q(I, \theta))_I.$$

For the second bracket,

$$p_R q_I - q_r p_I = (dRP, RQ_I) - (dRQ, RP_I) = (R^{-1}dRP, Q_I) - (R^{-1}dRQ, P_I),$$

where we changed the inner product notation to (\cdot, \cdot) . The presence of the

$R^{-1}dR$ implies left invariance. Using the correspondence (57), we get

$$\rho = dv \cdot \left\langle \sum_j P_j \times \partial/\partial I Q_j - Q_j \times \partial/\partial I P_j \right\rangle,$$

where \times is the vector product in \mathbb{R}^3 . In short notation,

$$\rho = dv \cdot \langle P \times Q_I - Q \times P_I \rangle.$$

It can also be written

$$\rho = dv \cdot \frac{\partial}{\partial I} \langle P \times Q \rangle = dv \cdot \frac{\partial}{\partial I} \langle -M \rangle,$$

as we wanted to prove. ■

Example: Hannay's Slowly Rotating Planar Hoop

A unit mass is travelling along a hoop $C : s \rightarrow (x(s), y(s))$ of length L . Action-angle coordinates are given by

$$\theta = \frac{2\pi s}{L}, \quad I = \frac{L\dot{s}}{2\pi}.$$

The hoop is slowly rotated through a full turn (parameter space $G = S^1$). Compute the geometric phase (the 2π factor in front is the integral over S^1):

$$\Delta\theta = 2\pi \frac{d}{dI} \frac{1}{2\pi} \int_0^{2\pi} (y\dot{x} - x\dot{y}) d\theta.$$

One gets

$$\begin{aligned} \Delta\theta &= 2\pi \frac{d}{dI} \frac{1}{L} \int_0^L (y\dot{x} - x\dot{y}) ds \\ &= 2\pi \frac{1}{L} \frac{d}{dI} \int_0^L (ydx - xdy) s \\ &= \left(\frac{2\pi}{L}\right)^2 \frac{d}{dI} \left[I \oint_C ydx - xdy \right] \end{aligned}$$

so that

$$\Delta\theta = -8\pi^2 \frac{A}{L^2},$$

where A is the area enclosed by the hoop. In terms of the arc length,

$$\Delta s = -4\pi \frac{A}{L}. \quad (58)$$

If C is a circle of radius r ,

$$[\Delta s]_{\text{circle}} = -2\pi r,$$

which is simply an artifact, since the origin of the arc length advances by $2\pi r$ as the hoop makes a circle. Thus we must add L to (58) to cure this "Jules Verne's syndrome":

$$\Delta s = L - 4\pi \frac{A}{L}, \quad (59)$$

which is ≥ 0 in view of the isoperimetric inequality.

9 The Main Theorem

The astute reader will suspect that something deeper is going on, involving the momentum map.

Theorem 9.1 *Let N a symplectic submanifold of a symplectic manifold M . Assume that a Lie group G acts symplectically on M with momentum map $J : M \rightarrow \mathcal{G}^*$. Fix a Lagrangian foliation on N . Then $\pi : G \cdot N \rightarrow G$ is a symplectic fiber bundle, and its torus subbundles \mathcal{T} (locally defined by fixing a set of action variables) are T^n fiber bundles over G . Moreover, the Hannay–Berry 1-form*

$$\rho(\xi) = \text{grad}_I \langle -J_\xi(I, \theta) \rangle \quad (60)$$

defines a parallel transport operator on the torus subbundles. The parallel transport does not depend on the choice of action-angle variables on N .

Exercise 9.2 *Prove Theorem 9.1 for $N = T^*S$, $M = T^*W$, where $S \subset W$. The Lie group G acts on W by isometries; the action is lifted to T^*W via $g \cdot p_q = (g \cdot q, (g^{-1})^* p_q)$.*

Hint. Take local coordinates (P, Q) on T^*S and action-angle coordinates $P = P(I, \theta)$, $Q = Q(I, \theta)$ such that $PdQ - Id\theta = dS(I, \theta)$. The

lifted action $p_q = g \cdot P_Q$ satisfies $pdq = PdQ$. Therefore, for the family of symplectic immersions $p = p(I, \theta, g)$, $q = q(I, \theta, g)$, we have

$$pd_{(I, \theta)} q - Id\theta = dS(I, \theta),$$

with generating function S independent of parameter $g \in G$. In particular, $\frac{\partial S}{\partial t} \equiv 0$. From Exercise 5.4 we get

$$\rho = \langle g, I \rangle dg = \text{grad}_I \langle -p_q \rangle dt,$$

where

$$p_q|_{t=0} = P \left(\frac{d}{dt} e^{t\xi} Q|_{t=0} \right) = J_\xi(P, Q), \quad \dot{g}(0) = \xi. \quad (61)$$

Problem 9.1 *Are there global obstructions to define the torus subbundles \mathcal{T} ?*

9.1 Invariance under a Maximal Torus T^r

The reader unfamiliar with Lie algebra theory can stick to $r = 1$, $T = S^1$, $G = SO(3)$. N is the phase space of a one- or two-degrees-of-freedom Hamiltonian with S^1 -symmetry. An extra degree of freedom is allowed, still maintaining integrability; there will be no holonomy for the latter angle. He or she can go directly to formula (63), and in the next section we compute the holonomy $\Delta\theta_1$ for several examples.

Suppose G is compact semisimple, acting on M with momentum map J . Suppose that N is invariant under the action of a maximal torus T^r of G , with $\dim N = 2r$ or $2(r+1)$. Choose a basis $\{\xi_i, \}_{i=1, \dots, \dim \mathcal{G}}$ of the Lie algebra with the first $\xi_1, \dots, \xi_r \in \mathfrak{t}^d$, the Lie algebra of T^r , the last ones in the Killing-perpendicular of $\mathfrak{t} \subset \mathcal{G}$.

Corollary 9.1 *The Berry–Hannay 1-form is*

$$\rho(\xi) = -\text{projection of } \xi \text{ overt}^r. \quad (62)$$

Proof. Choose action-angle variables for N such that the first r actions are

the momenta associated with $\xi_1, \dots, \xi_d \in t^r$:

$$J_{\xi_j} = I_j, \quad j = 1, \dots, r.$$

If $\dim N = 2r$, we have the Lagrangian foliation. If $\dim N = 2(r+1)$, complete the set of canonical coordinates for N with any pair of conjugate coordinates (I_{r+1}, θ_{r+1}) .

Claim. The average over T^r of the momenta associated with Lie algebra elements in the Killing-perpendicular of t^d is zero.

Then (62) follows immediately from (60). ■

Proof of the claim. Decompose ξ in (61) in its t^d component ξ and the Killing orthogonal component ζ . Use coordinates $(p(t), q(t), \theta(t))$ on N as above. By the equivariance of the momentum map, the claim boils down to the following fact from Lie group theory (see [1, section 4.10]):

Let ζ be in the Killing orthogonal to t^d . Then $\int_{T^r} Ad_g \zeta dg = 0$. ■

Remark 9.3 Impose no restrictions on $\dim N = 2(r+s)$. Introduce coordinates (p, q, I, θ) on N so that $\theta \in T^r$ corresponds to the maximal torus and I are the associated momenta as above. We have s extra degrees of freedom, q , with conjugate momenta p . A T^r invariant Hamiltonian on N writes as $H_o(p, q, I)$. In general, H_o is nonintegrable, but it has the invariant measure $d^s p \wedge d^s q \wedge d^r I \wedge d^r \theta$. Assuming ergodicity, an (even more) outrageous averaging principle can be invoked:

A perturbation $\epsilon H_1(p, q, I, \theta)$ can be replaced by its average along H_o .

Since $d^r \theta$ is a factor in the invariant measure, any perturbation whose average over T^r vanishes does not contribute (to first order) to the perturbed dynamics. In our case, we have the time-dependent Hamiltonian $H_o(g(et)^{-1} \cdot n)$ constrained to $g(et) \cdot N \subset M$. Using the symplectic coordinates (p, q, I, θ) , it writes as $H_o - \epsilon J_{g^{-1}g}$, where J is the momentum of the G -action on M . It is reasonable to conclude that (62) remains valid, and there is no holonomy for the (p, q) component.

Summarizing: Let $C : g = g(et)$ a curve in G (not necessarily closed). The non-vanishing geometric phases $\Delta\theta_i$, $i = 1, \dots, d$, associated with the maximal torus T^d are given by

$$\Delta\theta_i = -\text{proj}_{\xi_i} \int_C g^{-1} dg. \quad (63)$$

The integral $\int_C g^{-1} dg$ is the *hodograph* of $C \subset G$ to the Lie algebra \mathcal{G} .

9.2 Isotropic Oscillator

Let a planar isotropic harmonic oscillator or any one- or two-degrees-of-freedom system with S^1 symmetry be adiabatically transported along a curve C in \mathbb{R}^3 . Recall that the Frenet frame $R = (t, n, b)$ satisfies the Frenet-Serret equations

$$t' = \kappa n, \quad n' = -\kappa t + \tau b, \quad b' = -\tau n, \quad \left(' = \frac{d}{ds} \right),$$

which in our notation writes (using the correspondence (57)) as

$$R^{-1} dR \leftrightarrow (\tau, 0, \kappa) ds. \quad (64)$$

- If the oscillator is transported along the osculating plane (t, n) , then we project $R^{-1} dR$ on the third axis. Equation (63) gives

$$\Delta\theta = - \int_C \kappa ds. \quad (65)$$

- If the oscillator is transported along the normal plane (n, b) , we project over the first axis, so

$$\Delta\theta = - \int_C \tau ds. \quad (66)$$

This phenomenon has been observed in optical fibers (see [11]).

- For a surface curve, we use Darboux's frame $R = (t, n, N)$, where t is tangent to the curve and N is normal to the surface. The structure equations are $R^{-1} dR = (\tau_g, -\kappa_n, \kappa_g)$, where κ_n is the normal curvature, κ_g the geodesic curvature, and τ_g the geodesic torsion. If the system is transported along the tangent plane, then the holonomy is minus the total geodesic curvature along C . Using Gauss-Bonnet, we

get

$$\Delta\theta = - \int \kappa_g ds = -2\pi + \int \int K dS, \quad (67)$$

where K is the Gaussian curvature²⁰.

Exercise 9.4 *The term -2π is missing in Proposition 6.1. Is there a mistake?*

Answer. Both results are correct. We made two mistakes that cancelled out. In Proposition 6.1 we used the parallel-meridian frame on S^2 . β is singular at the poles, which produces an extra 2π (which we ignored there). Well, this oversight is compensated by Hopf's umlaufsatz (the tangent turns by 2π around a simple closed curve). Since the angle is measured from the tangent vector, a 2π should be discounted, which we did not do.

9.3 Foucault's Pendulum Revisited

We take the moving frame $(r(\varphi), R(\varphi))$ along the circle of latitude $\frac{\pi}{2} - \psi$.

Exercise 9.5 *Here $R^{-1}dR = (-\sin\psi, 0, \cos\psi)d\varphi$.*

Thus

$$\Delta\theta = -2\pi\cos\psi. \quad (68)$$

Exercise 9.6 *Transport adiabatically Hannay's top along the center circle of the Moebius strip.*

10 Final Remarks

At least two issues related to Corollary 9.1 may have disturbed the reader. First, it does not apply to our examples! $SE(3)$ is not compact, and the symplectic submanifold N is only invariant under $S^1 \times 0$, that is, if there is no translation part. Not to worry: by Theorem 8.1 the translation part $r(t) \in \mathbb{R}^3$ of $(r, R) \in SE(3)$ produces no holonomy. The reader should not

²⁰According to Klein [6], this result was first discovered by Radon as a "mechanical" demonstration of parallel transport.

have difficulty to modify the statement of Corollary 9.1 in order to handle these cases.

The second issue is not only embarrassing, it is actually frightening: our proof of Corollary 9.1 has a flaw when $\dim N = 2(r+1)!$ Given a T^r -invariant Hamiltonian $H_o(p, q, I)$, in general (as we observed in footnote 5) $\dot{\theta} = H_I(I, p, q) \neq \text{const.}$ We see that θ is not uniform in time (even if H is integrable). Retracing all logical steps to Theorem 9.1, we see that (in principle) we should replace θ by uniformizing variables, which we denote α . In other words, we should average over the latter, not over θ . What comes to our rescue is Remark 9.3. It is *declared* that time averages can be replaced by space averages with respect to the measure $dp \wedge dq \wedge d^r I \wedge d^r \theta$. A justification of this more general averaging principle is in order²¹.

To close this chapter, we list some examples, not discussed here for lack of space. They are discussed in our paper [7]. We leave them for further reading:

- slowly rotating elliptic billiard,
- rigid body with slowly changing inertia matrix,
- systems subjected to a strong constraining, nonhomogeneous, force,
- coupled slow-fast mechanical systems.

References

- [1] Adams, J. F., *Lectures on Lie Groups*, Benjamin, The University of Chicago Press, Chicago (1983).
- [2] Arnold, V., *Méthodes mathématiques de la mécanique classique*, MIR, Moscow (1978).
- [3] Duistermaat, J. J., *On global action angle coordinates*, Commun. Pure Appl. Math. **33**:6, 687-706 (1980).
- [4] Golin, S., Knauf, A., Marmi, S., *The Hannay angles: Geometry, adiabaticity and an example*, Commun. Math. Phys. **123**, 95-122 (1989).

²¹As far as we know, this has not been done by the experts in the analytic issues of Hamiltonian systems.

- [5] Hannay, J. H., *Angle variable holonomy in adiabatic excursion of an integrable hamiltonian*, J. Phys. A, **18**, 221–230 (1985).
- [6] Klein, F., *Vorlesungen über höhere Geometrie*, Grund. Math. Wiss. 22, Springer-Verlag, Berlin (1926).
- [7] Koiller, J., *Classical adiabatic angles for slowly varying mechanical systems*, Contemp. Math. **97**, 159–185 (1989).
- [8] Lochak, P., Meunier, C., *Multiphase Averaging for Classical Systems*, Springer-Verlag, New York (1988).
- [9] Montgomery, R., *The connection whose holonomy is the classical adiabatic angles of Hannay and Berry and its generalization to the non-integrable case*, Commun. Math. Phys. **120**, 269–294 (1988).
- [10] Neishtadt, A., *Averaging and passage through resonances*, in Proc. Intl. Congress Math., International Mathematical Union, Kyoto, 1271–1283 (1991).
- [11] Tomita, A, Chiao, R. Y., *Observation of Berry's topological phase by use of an optical fiber*, Phys. Rev. Lett. **57**, 937–940 (1986).
- [12] Weinstein, A., *Cohomology of symplectomorphism groups and critical values of hamiltonians*, Math. Z. **201**, 75–82 (1989).
- [13] Weinstein, A., *Connections of Berry and Hannay type for moving lagrangian submanifolds*, Adv. Math. **82**, 133–159 (1990).

Part 3: Holonomy for Gyrostats

11 The Hamiltonian

Let X, Y, Z be the principal axis of inertia of the carrier. For simplicity, consider just one flywheel on the Z -axis of the inertia ellipsoid of the main body. Let λ be the double eigenvalue of the flywheel inertia matrix, λ_3 its third eigenvalue; \mathcal{M} is the flywheel mass, $\dot{\theta}$ its angular velocity, and d the distance between the centers of mass of the carrier and flywheel.

Proposition 11.1 *The kinetic energy is a quadratic form in the Lie algebra $\mathbb{R} \times \mathfrak{so}(3)$, given by*

$$E = \frac{1}{2}(I\Omega, \Omega) + \frac{1}{2}(\lambda + \mathcal{M}d^2)(\Omega_1^2 + \Omega_2^2) + \frac{1}{2}\lambda_3\Omega_3^2 + \lambda_3\dot{\theta}\Omega_3 + \frac{1}{2}\lambda_3\dot{\theta}^2. \quad (69)$$

Denoting by I_1, I_2, I_3 the eigenvalues of I_{mb} , the inertia matrix of the main body,

$$E = \frac{1}{2}(\dot{\theta}, \Omega_1, \Omega_2, \Omega_3)I_g(\dot{\theta}, \Omega_1, \Omega_2, \Omega_3)^t, \quad (70)$$

where I_g , the inertia operator of the *gyrostat*, is given by

$$I_g = \begin{pmatrix} \lambda_3 & 0 & 0 & \lambda_3 \\ 0 & \lambda + \mathcal{M}d^2 + I_1 & 0 & 0 \\ 0 & 0 & \lambda + \mathcal{M}d^2 + I_2 & 0 \\ \lambda_3 & 0 & 0 & \lambda_3 + I_3 \end{pmatrix}.$$

Using the coordinates

$$\Omega_{\mathbf{g}} = (\dot{\theta}, \Omega_1, \Omega_2, \Omega_3)^t \quad (71)$$

for \mathcal{G} (Lie algebra of $S^1 \times SO(3)$) and

$$\mathbf{M}_{\mathbf{g}} = (I, M_1, M_2, M_3) \quad (72)$$

for its dual \mathcal{G}^* , it follows that the Legendre transformation is

$$\mathbf{M}_{\mathbf{g}} = I_g \Omega_{\mathbf{g}}. \quad (73)$$

Consider the pairing $\mathcal{G}^* \times \mathcal{G}$, given by $2h = (\mathbf{M}_{\mathbf{g}}, \Omega_{\mathbf{g}})$.

Proposition 11.2 *The energy of the gyrostat is expressed in terms of the momenta as*

$$h = (\mathbf{M}_g, I_g^{-1} \mathbf{M}_g). \quad (74)$$

Exercise 11.1 *Inverting I_g , obtain*

$$I_g^{-1} = \begin{pmatrix} \frac{1}{\lambda_3} + \frac{1}{I_3} & 0 & 0 & -\frac{1}{I_3} \\ 0 & \frac{1}{I_1 + \lambda + \mathcal{M}d^2} & 0 & 0 \\ 0 & 0 & \frac{1}{I_2 + \lambda + \mathcal{M}d^2} & 0 \\ -\frac{1}{I_3} & 0 & 0 & \frac{1}{I_3} \end{pmatrix}.$$

Moreover, since $\Omega_{\mathbf{g}} = I_g^{-1} \mathbf{M}_g$,

$$\Omega_1 = \frac{M_1}{I_1 + \lambda + \mathcal{M}d^2}, \quad \Omega_2 = \frac{M_2}{I_2 + \lambda + \mathcal{M}d^2}, \quad \Omega_3 = -\frac{1}{I_3} + \frac{M_3}{I_3}, \quad (75)$$

$$\dot{\theta} = \left(\frac{1}{I_3} + \frac{1}{\lambda_3} \right) I - \frac{1}{I_3} M_3. \quad (76)$$

Proposition 11.3

$$h = \frac{1}{2} \left(\frac{M_1^2}{I_1 + \lambda + \mathcal{M}d^2} + \frac{M_2^2}{I_2 + \lambda + \mathcal{M}d^2} + \frac{(M_3 - I)^2}{I_3} + \frac{I^2}{\lambda_3} \right). \quad (77)$$

Trajectories are intersections of a fixed momentum sphere $\|\mathbf{M}\| = J$ with the energy ellipsoids (77) with varying energies h , where I is taken as a parameter. The centers of the ellipsoids vary along the Z -axis. The possible phase portraits as a function of the parameter I are depicted in Figure 9.

Exercise 11.2 *Derive the Hamiltonian (69). See section 15 below.*

Is there a Poincaré description for gyrostats? The answer is “more or less,” since the invariable plane moves up and down and the herpolhodes are not planar curves.

Exercise 11.3 *Check this formula, which can be used to define the inertia ellipsoid:*

$$\alpha \Omega_1^2 + \beta \Omega_2^2 + \gamma \Omega_3^2 = 2h - \frac{I^2}{\lambda_3}, \quad (78)$$

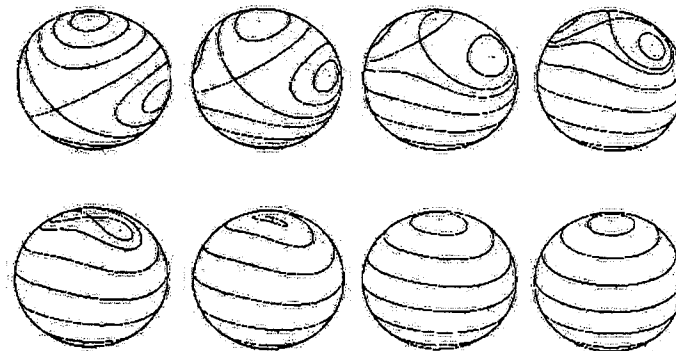


Figure 9. Reduced phase portrait for a rigid body with one flywheel. Top left: Euler system $I = 0$. For sufficiently big I , there are no unstable equilibria (bottom right). The satellite is then stabilized.

where

$$\alpha = I_1 + \lambda + \mathcal{M}d^2, \quad \beta = I_2 + \lambda + \mathcal{M}d^2, \quad \gamma = I_3. \quad (79)$$

Proposition 11.4 (*Modified Poincaré description*). *Replace the carrier by its inertia ellipsoid. After a polhode period T , the plane perpendicular to \mathbf{m} and touching the inertia ellipsoid attains the same height. In particular, the holonomy angle $\Delta\phi$ still makes sense.*

Proof. A short calculation gives

$$(\omega, \mathbf{M}) = \text{const.} + \Omega(t)I, \quad (80)$$

showing that the polhodes are planar curves only when $I = 0$. ■

12 Derivation of Formula (14)

We follow Montgomery's paper [15], pointing out the modifications where necessary.

12.1 Where and What to Integrate?

Configuration space is parametrized by three Euler angles

$$\varphi = \angle(x, \text{nodes}), \quad \psi = \angle(\text{nodes}, X), \quad \sigma = \angle(Z, z), \quad (81)$$

and one more angle θ , which gives the position of the flywheel.

Considering, on the Lie group $G = SO(3) \times S^1$, the left equivalence $T^*G \sim G \times \mathcal{G}^*$ gives the coordinates

$$(\varphi, \psi, \sigma, \theta, M_1, M_2, M_3, I).$$

We define an important closed curve $C = C_1 \cup C_2$, in a three-dimensional submanifold P of phase space $T^*(SO(3) \times S^1)$, fixing the constant values \mathbf{m}, I, h . Curve C_1 is described by the true dynamics in the interval $0 \leq t \leq T$, where T is the period of $\mathbf{M}(t)$ in the reduced dynamics; more precisely, C_1 is given by $(\varphi(t), \psi(t), \sigma(t), \theta(t), M(t), I)$.

For C_2 we fix $\mathbf{M}(t) = \mathbf{J}$ and $I(t) = I$, where without loss of generality, \mathbf{J} is taken parallel to $(0, 0, 1)$. The coordinates φ and θ vary from 0 to $\Delta\varphi$ and from 0 to $\Delta\theta$, respectively. The remaining variables are fixed. C_1 and C_2 meet at the starting and ending points.

Exercise 12.1 The action $p dq$ (canonical form defined on phase space) can be written as

$$pdq = (\mathbf{M}_g, d\Omega_g) = I d\theta + \mathbf{M} \cdot d\Omega. \quad (82)$$

Here $d\Omega$ is a vector of 1-forms. Find them²².

Hint. The calculations for $d\Omega$ are in [15].

12.2 Applying Stokes's Theorem

Consider any two-dimensional surface Σ in P bounded by C . We compute the line integral of $p dq$ along C and equate it with the integral of $d(p dq)$ over Σ .

²²To get the holonomy, one does not need the explicit expressions. The experts will tell you that the left and right "KAKS brackets" differ just in sign.

12.3 Line Integral over C_1

Since $(\mathbf{m}_g, \omega_g) = 2h$, we get

$$\int_{C_1} (\mathbf{m}_g, \omega_g) dt = 2hT. \quad (83)$$

12.4 Line Integral over C_2

Here we get one more term, besides the term $J\Delta\varphi$ in Montgomery's paper:

$$\int_{C_2} (I, 0, 0, J) \cdot (d\theta, 0, 0, d\varphi) = J\Delta\varphi + I\Delta\theta. \quad (84)$$

12.5 The Surface Integral over Σ

Actually, we compute the integral over the region $\Upsilon = \mathbf{M}(\Sigma)$, where $(\mathbf{M}, I) : T^*(SO(3) \times S^1) \rightarrow S^2 \times \mathbb{R}$. The first component \mathbf{M} sends rotation matrices R to points $R^{-1}\mathbf{J}$ of the sphere:

$$\iint_{\Sigma} d(pdq) = \iint_{\mathbf{M}(\Sigma)=\Upsilon} J d\Upsilon = J\Upsilon, \quad (85)$$

where Υ is the solid angle enclosed by the trajectory of the reduced system.

13 Holonomy for the Gyrostat

Using Stokes theorem and equations (83), (84), (85), we obtain

$$\Delta\varphi = \frac{2hT - I\Delta\theta}{J} - \Upsilon. \quad (86)$$

Observe that $\Delta\theta$ can be obtained by a quadrature using equation (76):

$$\Delta\theta = \int_0^T \dot{\theta}(t) dt = \left(\frac{1}{I_3} + \frac{1}{\lambda_3} \right) IT - \frac{1}{I_3} \int_0^T M_3(t) dt. \quad (87)$$

Remark 13.1 For the rigid body, Levi [10] made the beautiful observation that the polhode, viewed on the inertia ellipsoid, is transformed into the curve $\mathbf{M}(t)$ in the momentum sphere by Gauss's mapping of elementary differential geometry. This is the starting point of his derivation of the

holonomy formula²³. We have also extended this approach for gyrostats [5].

14 Final Remarks

Still another derivation of the holonomy for the rigid body follows from a general reconstruction formula, due to Marsden, Montgomery, and Ratiu [14], using connections on principal bundles.

In this example, the motion occurs simply by *inertia* in the configuration space of carrier *plus* flywheels. However, we can formulate an interesting *control problem*, where we allow “protooled” flywheel motions and we desire a prescribed carrier holonomy. We anticipate that two flywheels suffice to achieve any reorientation.

Problem: Locate the flywheels optimally and find the optimal flywheel motions $\dot{\theta}_i(t)$ to achieve the desired reorientation. For instance, if we have one flywheel, located in the Z -axis, we get the following time-dependent Lagrangian on $TSO(3)$:

$$E = \frac{1}{2}(I\Omega, \Omega) + \frac{1}{2}(\lambda + Md^2)(\Omega_1^2 + \Omega_2^2) + \frac{1}{2}\lambda_3\Omega_3^2 + \lambda_3\dot{\theta}\Omega_3. \quad (88)$$

Notice the presence of the control variable $\dot{\theta}$ in the last term.

Another classic example is Kirchhoff’s problem of the motion of a solid body through incompressible, inviscid, irrotational fluid. Here one has geodesic motions of a left-invariant metric on the group of rigid motions of three-dimensional space. The problem has six degrees of freedom; it is nonintegrable except at exceptional cases. See [2] and references therein. It would be instructive to compute the relevant holonomies for the integrable cases and to see what happens in the nearly integrable situations. A novel feature here is the possibility of *translational holonomy*, that is, how much the rigid body translates after one period of a periodic orbit of the reduced problem.

²³Reasoning in reverse, Levi gave a “mechanical proof” for the Gauss–Bonnet theorem [11].

15 Derivation of the Hamiltonian

Following Arnold [3], we use the following conventions for reference frames and vectors: corresponding vectors in frames K and k will be denoted by the same letter, capitalized in the former. Thus:

$\mathbf{q} \in k$ represents a point of the body viewed in space.

$\mathbf{Q} \in K$ is the same point viewed in the body frame. $\mathbf{q} = R\mathbf{Q}$.

$\mathbf{v} = \dot{\mathbf{q}} \in k$ is the velocity vector.

$\mathbf{V} \in K$ is the same vector, but viewed in the body frame. $\mathbf{v} = R\mathbf{V}$.

$\omega \in k$ is the angular velocity viewed “from space.”

$\Omega \in K$ is the angular velocity viewed “from the body.” $\omega = R\Omega$.

$\mathbf{m} \in k$ is the angular momentum viewed from space.

$\mathbf{M} \in K$ the angular momentum viewed from the body. $\mathbf{m} = R\mathbf{M}$.

Let f be the isomorphism between skew symmetric matrices and vectors in \mathbb{R}^3 , $f: \mathcal{A} \rightarrow \mathbb{R}^3$, $f(A_w) = \mathbf{w} = (w_1, w_2, w_3)$, $\mathbf{w} \in \mathbb{R}^3$, where

$$A_w = \begin{pmatrix} 0 & -w_3 & w_2 \\ w_3 & 0 & -w_1 \\ -w_2 & w_1 & 0 \end{pmatrix}, \quad A_w \in \mathcal{A}.$$

We denote the vector product with the same symbol $[\cdot, \cdot]$ as commutators of matrices. We have a Lie algebra isomorphism, namely,

$$f([A, B]) = [f(A), f(B)].$$

Contribution of the Carrier

$$\begin{aligned} E_{\text{carrier}} &= \frac{1}{2} \sum_i \mu v_i^2 \\ &= \frac{1}{2} \sum_i \mu V_i^2 \end{aligned}$$

$$\begin{aligned}
&= \frac{1}{2} \sum_i \mu([\Omega, \mathbf{Q}_i])^2 \\
&= \frac{1}{2} \sum \mu([\Omega, \mathbf{Q}_i], [\Omega, \mathbf{Q}_i]) \\
&= \frac{1}{2} \sum \mu([\mathbf{Q}_i, [\Omega, \mathbf{Q}_i], \Omega]) \\
&= \frac{1}{2} \sum_i (\mathbf{M}_i, \Omega) \\
&= \frac{1}{2} (\mathbf{M}, \Omega) \\
&= \frac{1}{2} (I\Omega, \Omega).
\end{aligned}$$

Here, as in the case of the usual free rigid body, we can assume that the positive definite symmetric matrix I is in diagonal form.

Contribution of the Flywheel

A point in the flywheel is written as

$$\mathbf{q} = RG\tilde{\mathbf{Q}} + R\mathbf{P}.$$

Differentiating, we get

$$\begin{aligned}
\dot{\mathbf{q}} &= \dot{R}(G\tilde{\mathbf{Q}}) + R(G\dot{\tilde{\mathbf{Q}}}) + \dot{R}\mathbf{P} \\
&= (\dot{R}R^{-1})RG\tilde{\mathbf{Q}} + R(\dot{G}\tilde{\mathbf{Q}} + G\dot{\tilde{\mathbf{Q}}}) + \dot{R}R^{-1}\mathbf{p} \\
&= \dot{R}R^{-1}(\mathbf{q} - \mathbf{p}) + R(\dot{G}G^{-1})G\tilde{\mathbf{Q}} + \dot{R}R^{-1}\mathbf{p}.
\end{aligned}$$

Therefore,

$$\dot{\mathbf{q}} = [\omega, \mathbf{q} - \mathbf{p}] + R[\Theta, (\mathbf{Q} - \mathbf{P})] + [\omega, \mathbf{p}].$$

where $\Theta = f(\dot{S}S^{-1})$, $\tilde{\Theta} = f(S^{-1}\dot{S})$. Let E_{cat} be the kinetic energy of the flywheel. Then we have:

$$\begin{aligned}
E_{cat} &= \sum \frac{1}{2} \mu([\omega, \mathbf{q} - \mathbf{p}], [\omega, \mathbf{q} - \mathbf{p}]) \\
&\quad + \sum \mu([\omega, \mathbf{q} - \mathbf{p}], R[\Theta, \mathbf{Q} - \mathbf{P}]) \\
&\quad + \sum \frac{1}{2} \mu([\omega, \mathbf{p}], [\omega, \mathbf{p}]) \\
&\quad + \sum \frac{1}{2} \mu(R[\Theta, \mathbf{Q} - \mathbf{P}], R[\Theta, \mathbf{Q} - \mathbf{P}])
\end{aligned}$$

$$\begin{aligned}
&+ \sum \mu([\omega, \mathbf{q} - \mathbf{p}], [\omega, \mathbf{p}]) \\
&+ \sum \mu(R[\Theta, \mathbf{Q} - \mathbf{P}], [\omega, \mathbf{p}]).
\end{aligned}$$

Calculations in a Particular Case

For simplicity, we place the flywheel to the Z -axis of the inertia ellipsoid of the main body. Clearly, the inertia operator of the flywheel alone in the base \tilde{K} (I_{cat}) is diagonal, with two equal eigenvalues (λ) and one possibly distinct (λ_3). The equality of the first two eigenvalues reflects the *material symmetry* of the flywheel implying that

$$GI_{cat}G^{-1} = I_{cat}.$$

This is true because G is a matrix of the type

$$\begin{pmatrix} \cos \theta t & -\sin \theta t & 0 \\ \sin \theta t & \cos \theta t & 0 \\ 0 & 0 & 1 \end{pmatrix}.$$

Thus $\Theta = f(G^{-1}\dot{G}) = \dot{\theta}(0, 0, 1)$.

Nonvanishing Terms

$$\begin{aligned}
\sum \frac{1}{2} \mu([\omega, \mathbf{q} - \mathbf{p}], [\omega, \mathbf{q} - \mathbf{p}]) &= \sum \frac{1}{2} \mu([\Omega, \mathbf{Q} - \mathbf{P}])^2 \\
&= \sum \frac{1}{2} \mu([\mathbf{Q} - \mathbf{P}, [\Omega, \mathbf{Q} - \mathbf{P}], \Omega]) \\
&= \frac{1}{2} (GI_{cat}G^{-1}\Omega, \Omega) \\
&= \frac{1}{2} \lambda (\Omega_1^2 + \Omega_2^2) + \frac{1}{2} \lambda_3 \Omega_3^2.
\end{aligned}$$

From (89), we get

$$\begin{aligned}
\sum \mu([\omega, \mathbf{q} - \mathbf{p}], R[\Theta, \mathbf{Q} - \mathbf{P}]) &= \sum \mu([\Omega, \mathbf{Q} - \mathbf{P}], [\Theta, \mathbf{Q} - \mathbf{P}]) \\
&= \sum \mu([\mathbf{Q} - \mathbf{P}, [\Theta, \mathbf{Q} - \mathbf{P}], \Omega])
\end{aligned}$$

$$\begin{aligned}
&= (I_{cat} \Theta, \Omega) \\
&= (\Omega, \lambda_3 \Theta) \\
&= \lambda_3 \Omega_3 \dot{\theta}.
\end{aligned}$$

On the other hand, since $|\mathbf{P}| = d$, it follows that

$$\begin{aligned}
\sum \mu([\omega, \mathbf{p}], [\omega, \mathbf{p}]) &= \frac{1}{2} \mathcal{M}(\|\Omega\|^2 \|\mathbf{P}\|^2 - (\Omega, \mathbf{P})^2) \\
&= \frac{1}{2} \mathcal{M}\{(\Omega_1^2 + \Omega_2^2 + \Omega_3^2)d^2 - \Omega_3^2 d^2\} \\
&= \frac{1}{2} \mathcal{M}d^2(\Omega_1^2 + \Omega_2^2),
\end{aligned}$$

where \mathcal{M} is the mass of the flywheel. Finally, we obtain an expected term. Developing (89) in detail, we get:

$$\begin{aligned}
\sum \frac{1}{2} \mu(R[\Theta, \mathbf{Q} - \mathbf{P}], R[\Theta, \mathbf{Q} - \mathbf{P}]) &= \sum \frac{1}{2} \mu([\Theta, \mathbf{Q} - \mathbf{P}], [\Theta, \mathbf{Q} - \mathbf{P}]) \\
&= \sum \frac{1}{2} \mu(\mathbf{Q} - \mathbf{P}, [\Theta, \mathbf{Q} - \mathbf{P}], \Theta) \\
&= \frac{1}{2} (I_{cat} \Theta, \Theta) \\
&= \frac{1}{2} (\lambda_3 \Theta, \Theta) \\
&= \frac{1}{2} \lambda_3 \dot{\theta}^2.
\end{aligned}$$

Vanishing Terms

Since the center of mass of the flywheel is located at $\mathbf{P} \in K$, we have $\tilde{\mathbf{P}} = 0$. Thus, from (89) we conclude that:

$$\begin{aligned}
\sum \mu([\omega, \mathbf{q} - \mathbf{p}], [\omega, \mathbf{p}]) &= \sum \mu([\Omega, \mathbf{Q} - \mathbf{P}], [\Omega, \mathbf{P}]) \\
&= \sum \mu([\mathbf{Q} - \mathbf{P}, \Omega], [\mathbf{P}, \Omega]) \\
&= \sum \mu(\mathbf{P}, [\Omega, [\mathbf{Q} - \mathbf{P}, \Omega]]) \\
&= \mathcal{M}(\mathbf{P}, [\Omega, [G\tilde{\mathbf{P}}, \Omega]]) \\
&= 0.
\end{aligned}$$

Similarly,

$$\begin{aligned}
\sum \mu(R[\Theta, \mathbf{Q} - \mathbf{P}], [\omega, \mathbf{p}]) &= \sum \mu([\Theta, \mathbf{Q} - \mathbf{P}], [\Omega, \mathbf{P}]) \\
&= \mathcal{M}([\Theta, G\tilde{\mathbf{P}}], [\Omega, \mathbf{P}]) \\
&= 0.
\end{aligned}$$

Contribution of the Flywheel

Summarizing our calculations,

$$\begin{aligned}
E_{flywheel} &= \frac{1}{2} \lambda_3 \dot{\theta}^2 \\
&\quad + \frac{1}{2} (\lambda + \mathcal{M}d^2) (\Omega_1^2 + \Omega_2^2) \\
&\quad + \frac{1}{2} \lambda_3 \Omega_3^2 \\
&\quad + \lambda_3 \dot{\theta} \Omega_3.
\end{aligned}$$

References

- [1] Abraham, R., Marsden, J. E., *Foundations of Mechanics*, Addison-Wesley, Boston (1978).
- [2] Aref, H., Jones, S. W., *Chaotic motion of a solid through ideal fluid*, Phys. Fluids A 5, 3026–3028 (1993).
- [3] Arnold, V. I., *Mathematical Methods of Classical Mechanics*, Springer-Verlag, New York (1978).
- [4] Bloch, A., Krishnaprasad, P. S., J. Marsden, J. E., Sanchez de Alvarez, G., *Stabilization of rigid body dynamics by internal and external torques*, Automatica 28, 745–746 (1994).
- [5] Almeida, M. L. B. P., *Holonomias para corpos rígidos e girostatos*, M.Sc. thesis, Instituto de Matemática, Universidade Federal do Rio de Janeiro (1993).
- [6] Goldstein, H., *Classical Mechanics*, Addison-Wesley, Boston (1980).
- [7] Hubert, C. H., *An attitude acquisition technique for dual-SPIN spacecraft*, Ph.D thesis, Cornell University, Ithaca, NY (1980).

- [8] Landau, L., E. Lifchitz, E., *Mécanique*, MIR, Moscow (1966).
- [9] Leimanis, E., *The General Problem of the Motion of Coupled Rigid Bodies about a Fixed Point*, Springer-Verlag, New York (1965).
- [10] Levi, M., *Geometric phases in the motion of rigid bodies*, Arch. Rational Mech. Anal. **122**, 213–229 (1993).
- [11] Levi, M., A “bicycle wheel” proof of the Gauss–Bonnet theorem, dual cones and some mechanical manifestations of the Berry phase, Expos. Math. **12**, 145–164 (1993).
- [12] Krishnaprasad, P. S., *Lie Poisson structures on dual spin spacecraft and asymptotic stability*, Nonlinear Anal. **9**:10, 1011–1035 (1985).
- [13] Marsden, J. E., *Lecture Notes on Mechanics*, London Math. Soc. Lect. Notes Series vol. **174**, Cambridge University Press, Cambridge, UK (1992).
- [14] Marsden, J. E., Montgomery, R., Ratiu, T., *Reduction, symmetry, and phases in mechanics*, Mem. Amer. Math. Soc. **88**, 436 (1990).
- [15] Montgomery, R., *How much does the rigid body rotate? A Berry’s phase from the 18th century*, Amer. J. Phys. **59**, 394–398 (1991).
- [16] Wittenburg, J., *Dynamics of Systems of Rigid Bodies*, B.G. Teubner, Stuttgart (1977).

Part 4: Microswimming

The lives of protozoa and bacteria may be unfamiliar to us “higher” forms of life, and therefore dismissed as uninteresting. We should not be so arrogant: as Stephen Jay Gould says, to bacteria, we are mountains full of exploitable goodies. They are much better fit for survival!

*E. coli*²⁴, the most common intestinal bacteria, are approximately 2×10^{-4} cm in length and 10^{-4} cm wide. They have six flagellar filaments emerging from random points on the cell body. At such microscopic sizes, water is so viscous that inertia plays no role.

Reynolds number, given by

$$R_e = LV/\mu = \frac{\text{Inertial Forces}}{\text{Viscous Forces}}, \quad (89)$$

where L , V , μ are, respectively, a characteristic length, velocity, and kinematic viscosity, measures the relative importance of inertia to viscosity in fluid dynamical problems. If $R_e \ll 1$, viscosity effects dominate. Reynolds number for swimming microorganisms is typically between 10^{-2} for protozoa and 10^{-5} for motile bacteria. They propel themselves in an inertialess environment.

“*Earnest*” teaches many lessons to the biologist, to the mechanical or electrical engineer, and even to the psychologist. *E. coli* moves in a “biased” random way: runs alternating with tumbles. In a favorable direction, the runs are statistically longer. But the runs are not shorter in a bad direction, so *Earnest* is an optimist. For the basic biophysics of microswimming, see E. Purcell’s beautiful talk, “Life at Low Reynolds number” [19] and Berg’s book, *Random Walks in Biology* [1].

Here are some strategies observed in nature:

- *E. coli* swim using helical propellers that rotate.
- Small nematodes and spermatozoan tails swim using planar undulations.
- *Spirochetes* swim using internal flagella.
- *Synechococcus* swim using traveling compression waves.

²⁴*E.* stands for Escherichia, but we prefer rather *Earnest*.

- Many protozoa swim by waving a layer of densely packed cilia (Figure 10).

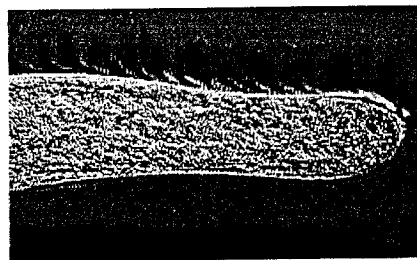


Figure 10. Metacrony in *Spirostomum*. Cilia work in coordination through a space-temporal wave along the cell surface (Dusenbery [6]).

16 Historical Remarks

The implications of low Reynolds number for microswimming were realized only in 1930 (Ludwig [17]). Perturbation methods were used by Taylor ([21], 1951) in his treatment of the infinite swimming sheet. This problem was also discussed in Blake ([4], 1971), and Childress ([5], 1981). Lighthill ([16], 1952) calculated the swimming velocity of a squirming spherical cell. Blake [2] corrected some of Lighthill's formulas and adapted Lighthill's model to explain ciliary propulsion by replacing the loci of the cilia tips by a continuous envelope. For certain densely ciliated organisms, such as *Opalina*, this model provides good results.

Blake ([4], 1971) discussed the problem of swimming in two dimensions. The swimming velocity of a cell with circular geometry, due to small amplitude, symmetric traveling waves was approximated using perturbation techniques. Shapere and Wilczek ([20], 1989) interpreted the problem in differential geometric terms, namely, as a connection on a principal bundle. This description places the problem in a broader class of kinematical problems that includes satellite reorientation and the ability of a falling cat to land on her feet (Montgomery 1990, [18]).

17 The Configuration Space

The configuration space, which we will denote by \mathcal{Q} , describes the organism in its environment and is the space of all parametrized embeddings $q : S^2 \rightarrow \mathbb{R}^3$. The image $\Sigma = q(S^2)$ represents the outer membrane of the organism or the ciliary "envelope,"²⁵ and will be referred to as a "located shape." It is important to keep in mind that q is a *parametrized* embedding: reparametrizations of the *same* geometric shape represent *different* states of the organism²⁶.

By composition on the image, there is a left action on \mathcal{Q} by the group $SE(3)$ of Euclidean motions

$$SE(3) \curvearrowright \mathcal{Q} \rightarrow S. \quad (90)$$

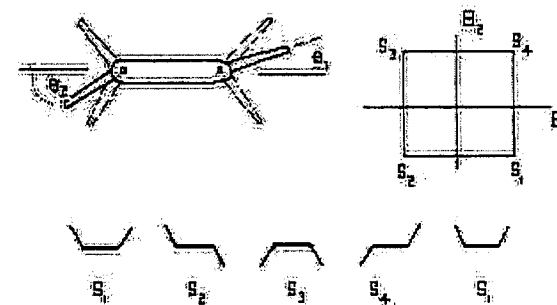


Figure 11. In what direction will Purcell's *animat* go? See [19].

The base space of the bundle is $S = \mathcal{Q}/SE(3)$, the space of "unlocated shapes." The tangent space $T_q\mathcal{Q}$ at an embedding $\Sigma = q(S^2)$ consists of all vector fields along Σ ,

$$\vec{v} : \Sigma \rightarrow \mathbb{R}^3, \quad (91)$$

and represents an infinitesimal boundary motion. Purcell's "cult paper" [19] has a delightful example with a challenge to the reader; see Figure 11.

²⁵Flagellary motion can also be studied, using techniques from slender body theory.

²⁶Certain organisms (e.g., *synechococcus*) are thought to swim using what can be mathematically described as time-dependent self-reparametrizations: traveling compression and expansion waves along the outer membrane [8].

The two most important features are the following:

- \mathcal{Q} possesses a very natural Riemannian metric, given by the hydrodynamical power expenditure. Remarkably, the physical constraints for self-locomotion, namely, no net force or torque being exerted on the fluid, coincide with the horizontal spaces of the associated mechanical connection A .
- Swimming velocity is computed in terms of the *curvature* coefficients via the small amplitude approximation (104) given below.

To compute the curvature for a specific shape, we need the following ingredients:

- Solutions to Stokes equations with boundary conditions specified on the base shape.
- An expression for the Lie bracket of these vector fields in the exterior of the shape.
- An expression for the connection form A .
- A splitting of the basis vectors into horizontal and vertical.

This program was started by our group in the papers [11, 12, 13, 14]. Collaborations for future work are welcome. The horizontal distributions for the indicated geometries can be inferred from the work by the following authors:

	Geometry	Restrictions
Taylor (1951) [21]	Planar	Axially symmetric
Lighthill (1952) [16]	Spherical	Axially symmetric
Blake (1970)	Spherical, circular, and cylindrical	Axially symmetric
Shapere-Wilczek (1989) [20]	Spherical and circular	None
Ehlers (1995)	Elliptical	None

18 Hydrodynamics

Navier–Stokes equations (without body forces) are given by

$$\nabla \cdot \hat{v} = 0, \quad \rho \frac{D\hat{v}}{Dt} = -\nabla p + \mu \nabla^2 \hat{v}, \quad (92)$$

where ρ is the density and \hat{v} , p the velocity and pressures of the fluid external to the organism described by the shape $\Sigma \in \mathcal{Q}$.

In the Stokesian realm where inertial effects are neglected, we use the Stokes approximation. These linear partial differential equations of elliptic type are

$$\nabla \cdot \hat{v} = 0, \quad -\nabla p + \mu \nabla^2 \hat{v} = 0. \quad (93)$$

The nonslip assumption gives the boundary condition $\vec{v} \in T_{\Sigma} \mathcal{Q}$, defining a unique solution, which we denote (Σ, \hat{v}, p) .

Exercise 18.1 Recall that the group of Euclidean motions acts on \mathcal{Q} . Let R be a rotation matrix, then whenever $\hat{v}(\vec{r})$, $p(\vec{r})$ is a solution with prescribed boundary values at Σ , $R^T \hat{v}(R\vec{r} + \vec{b})$, $p(R\vec{r} + \vec{b})$ is also a solution with prescribed values on $R\Sigma + \vec{b}$.

Remark 18.2

- (i) At each instant the neutrally buoyant, low Reynolds number swimmer does not exert zero net forces and torques on the fluid [5]. The inertial terms in the equations of motion that would account for such an imbalance are not present (the nonlinear terms in the Navier–Stokes equations). It is this condition that will define a geometrical connection on the space of located shapes.
- (ii) Because acceleration does not play a role, the equations of motion are time independent. The boundary condition depends on time, but the fluid velocities depend only on the instantaneous boundary velocity field. A given change in shape leads to an instantaneous motion through the whole fluid no matter how fast it is carried out (so long as R_e remains $\ll 1$).
- (iii) The “scallop theorem” [19]: because of time independence, reciprocal motions lead to no net translation. Stokes flows are reversible: one

can stir then unstir fluids if $Re \ll 1!!!$ There are no low Reynolds number "scallop"; low Reynolds number swimmers must have at least two-degrees of freedom.

The stress tensor σ is given by

$$\sigma_{ij} = -p\delta_{ij} + \mu \left(\frac{\partial u_i}{\partial x_j} + \frac{\partial u_j}{\partial x_i} \right). \quad (94)$$

Exercise 18.3 Show, from Stokes equations, that the stress tensor σ is divergence-free.

Given any mathematical surface S outside Σ with normal \vec{n} , one computes the field of surface forces (stresses) along S :

$$\vec{f} = \sigma(\hat{v}) \cdot \vec{n}.$$

The classic "Lorentz reciprocity theorem" [9] says that the operator

$$\vec{v} \rightarrow \vec{f}$$

on the space of vector fields along Σ is self-adjoint and positive. Hence we have the following definition.

Definition 18.4 The hydrodynamical power dissipation

$$P = \int_{\Sigma} \vec{f} \cdot \vec{v} \, dS$$

defines a Riemannian metric on \mathcal{Q} , which we call the power metric.

19 The Momentum Mapping

Proposition 19.1 The momentum map $\mu: T\mathcal{Q} \rightarrow se(3)^*$ is given by

$$\begin{aligned} \mu(\vec{v}_{\Sigma}) \cdot (\vec{w}, \vec{b}) &= \vec{w} \cdot \int_{\Sigma} \vec{r} \times \sigma(\hat{v}) \cdot \vec{n} \, dS + \vec{b} \cdot \int_{\Sigma} \sigma(\hat{v}) \cdot \vec{n} \, dS \\ &= \vec{w} \cdot \int_{\Sigma} \vec{r} \times \vec{f} \, dS + \vec{b} \cdot \int_{\Sigma} \vec{f} \, dS = \vec{w} \cdot \vec{T} + \vec{b} \cdot \vec{F}, \end{aligned} \quad (95)$$

where we have represented an element of $se(3)$ as a pair of vectors (\vec{w}, \vec{b}) . Here $\vec{F} = \int_{\Sigma} \vec{f} \, dS$ is the total force, and $\vec{T} = \int_{\Sigma} \vec{r} \times \vec{f} \, dS$ is the total torque.

Exercise 19.1 Prove this formula, using the abstract nonsense definition (16). The identification $T\mathcal{Q} \cong T^*\mathcal{Q}$ is given by the power metric

$$\langle \vec{v}, \vec{w} \rangle = \int_{\Sigma} \vec{v} \cdot \sigma(\hat{w}) \vec{n} \, dS.$$

Hint. For any element $\xi = (\vec{w}, \vec{b}) \in se(d)$ of the Lie algebra, ξ_P is an infinitesimal rigid motion of the shape Σ and is described by the rigid motion vector field, $\xi_P(\Sigma) = (\vec{w} \times \vec{r} + \vec{b})|_{\Sigma}$. Therefore,

$$\begin{aligned} \mu(\vec{v}_{\Sigma}) \cdot (\vec{w}, \vec{b}) &= \int_{\Sigma} (\vec{w} \times \vec{r} + \vec{b}) \cdot \sigma(\hat{v}) \vec{n} \, dS \\ &= \int_{\Sigma} (\vec{w} \times \vec{r}) \cdot \sigma(\hat{v}) \vec{n} \, dS + \int_{\Sigma} \vec{b} \cdot \sigma(\hat{v}) \vec{n} \, dS \\ &= \vec{w} \cdot \int_{\Sigma} \vec{r} \times \sigma(\hat{v}) \vec{n} \, dS + \vec{b} \cdot \int_{\Sigma} \sigma(\hat{v}) \vec{n} \, dS. \end{aligned}$$

Exercise 19.2 Since σ is divergence-free, the total force and the total torque can be computed by integrating along any other mathematical surface surrounding Σ .

Remark 19.3 The power metric is degenerate in dimension $d = 2$. In fact, the Stokes paradox says that there is no Stokesian flow vanishing at infinity for a uniformly translating cylinder, or, what is the same, there is no Stokesian flow past a cylinder that is uniform at infinity. One can remedy this by admitting flows with logarithmical singularities at infinity, but we do not pursue this approach. Rather, in two dimensions we admit that for translations of a shape $\vec{v} = \vec{b}$, its Stokes extension is $\hat{v} = \vec{b}$, in which the fluid moves rigidly as a whole with constant pressure $p \equiv 0$. It follows that $\langle \vec{v}, \vec{b} \rangle = 0$ for all \vec{v} . In other words, the Legendre transform that associates forces to velocities has a nontrivial kernel generated by the rigid translations.

Definition 19.4 Vertical vector fields are those generated by infinitesimal rigid motions of the shape, and horizontal vector fields form the orthogonal complement to the vertical space, with respect to the power metric.

Proposition 19.2 For $d = 3$, a vector \vec{v}_Σ is horizontal if and only if $\mu(\vec{v}_\Sigma) = 0$. For $d = 2$, \vec{v}_Σ is horizontal if and only if \vec{v} is not a rigid translation and $\mu(\vec{v}_\Sigma) = 0$.

The following result is very useful for the calculations.

Proposition 19.3 In order to compute the momentum map, it is enough to find the Stokes extension of a finite number of boundary vector fields, namely, those given by infinitesimal rigid motions $\vec{w} \times \vec{r} + \vec{b}$.

Proof. Let \hat{b} and \hat{w} denote the Stokes extensions of translations and rotations, respectively. First we consider translations

$$\mu(\vec{v})(\vec{0}, \vec{b}) = \vec{b} \cdot \int_{\Sigma} \sigma(\hat{v}) \cdot \vec{n} dS = \int_{\Sigma} \vec{b} \cdot \sigma(\hat{v}) \cdot \vec{n} dS = \int_{\Sigma} \vec{v} \cdot \sigma(\hat{b}) \cdot \vec{n} dS,$$

and similarly for the rotations,

$$\begin{aligned} \mu(\vec{v})(\vec{w}, \vec{0}) &= \vec{w} \cdot \int_{\Sigma} \vec{r} \times \sigma(\hat{v}) \cdot \vec{n} dS = \int_{\Sigma} \vec{w} \cdot (\vec{r} \times \sigma(\hat{v}) \cdot \vec{n}) dS \\ &= \int_{\Sigma} (\vec{w} \times \vec{r}) \cdot \sigma(\hat{v}) \cdot \vec{n} dS = \int_{\Sigma} \vec{v} \cdot \sigma(\hat{w}) \cdot \vec{n} dS. \end{aligned}$$

Definition 19.5 Take a basis \vec{v}_k , $k = 1, \dots, 6$ for the vertical vector fields, that is, the three unit translations and the three unit infinitesimal rotations. The 6×6 matrix I with entries $\langle \vec{v}_i, \vec{v}_j \rangle$ is called in fluid dynamics the resistance matrix. In our language it corresponds to the locked inertia tensor.

Decompose \vec{v} into its horizontal and vertical parts, $\vec{v} = \vec{v}^h + \vec{v}^v$. Write $\vec{v}^v = \sum c_k \vec{v}_k$ so that

$$0 = \langle \vec{v}^h, \vec{v}_l \rangle = \langle \vec{v}, \vec{v}_l \rangle - \langle \vec{v}^v, \vec{v}_l \rangle = \langle \vec{v}, \vec{v}_l \rangle - \sum c_k \langle \vec{v}_k, \vec{v}_l \rangle.$$

Therefore,

$$\begin{aligned} I(\vec{v}^v) \cdot \vec{v}_l &= \sum c_k I(\vec{v}_k) \cdot \vec{v}_l \\ &= \langle \vec{v}, \vec{v}_l \rangle, \end{aligned}$$

which says that

$$I_{\Sigma}(\vec{v}^v) = \langle \vec{v}, \cdot \rangle = \mu(\vec{v}).$$

In the case $d = 3$, I is invertible and so

$$(\vec{b}, \vec{w}) = A(\vec{v}) = I^{-1}(\mu(\vec{v})). \quad (96)$$

Definition 19.6 The Stokes extension $\vec{v}_{(\vec{b}, \vec{w})}$ associated to the rigid motion (\vec{b}, \vec{w}) ($= A(\vec{v})$) is called the counterflow of the velocity field \vec{v} .

In practice, we search for a counterflow with boundary condition (\vec{b}, \vec{w}) whose Stokes resistance $I((\vec{b}, \vec{w}))^\dagger$ equals $\mu(\vec{v})$. Then we subtract:

$$\vec{v} - \vec{v}_{(\vec{b}, \vec{w})} \text{ is horizontal.}$$

How about the curvature of the connection? There is a beautiful “master formula” by Shapere and Wilczek [20], derived more rigorously in Ehlers’ thesis [7]:

$$\mathcal{F}_{\Sigma}(\vec{u}, \vec{v}) = A([\vec{v}^h, \vec{u}^h]), \quad (97)$$

where $[\cdot, \cdot]$ is the Lie bracket of vector fields.

Exercise 19.7 Prove the “master formula” (97).

Hint. Start with Cartan’s formula $d\omega(u_o, v_o) = v \cdot \omega(u) - u \cdot \omega(v) - \omega[u, v]$ for the exterior derivative of a 1-form on a manifold Q . Recall that in the right-hand side, u and v are arbitrary extensions of vectors $u_o, v_o \in T_q Q$. Using the solution of the Stokes equations, extend the tangent vector $\vec{v}_m^h \in T_{\Sigma} Q$ to a neighborhood of Σ . Since the stress tensor is divergence-free, the Stokes extension of the horizontal projection \vec{v}^h at the shape Σ remains horizontal for deformed shapes $\Sigma(t)$. Hence the first two terms in Cartan’s formula vanish. It remains to show that the Lie bracket of vector fields in the infinite-dimensional manifold Q can be computed using the familiar Lie bracket of vector fields²⁷. ■

Exercise 19.8 What is needed from fluid mechanics in order to study motions due to self-reparametrizations of Σ (vector fields tangent to Σ)?

²⁷This is so plausible that it could remain unnoticed, but proving this fact requires some abstract thinking.

Solution. In (97) the Lie bracket of tangential vector fields does not require the Stokes extensions. So fluid mechanics enters (i) to obtain the resistance matrix I , and (ii) to find total force and torque for a given tangential vector field. Figure 12 and 13 explain qualitatively the counterintuitive fact that the motion of the organism is in the same direction as the waves of contraction/expansion.

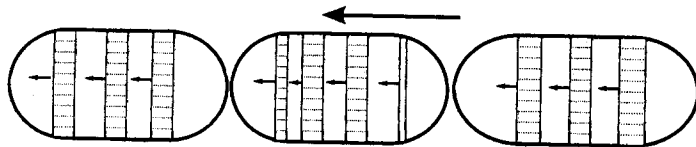


Figure 12. The tangential traveling wave mechanism. The black and white areas represent regions of contraction and expansion on the cell's outer membrane. The cell travels in the same direction of the wave.

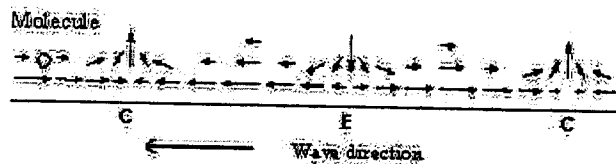


Figure 13. What happens to the test molecule? The wave train moves to the left. The molecule tends to move more to the right than to the left. Why? Explain qualitatively.

Exercise 19.9 (Lighthill's *Fugo* [12]). Consider a spherical cell of radius r_1 that draws an angle of $\delta\phi$ of its outer membrane towards one pole, shrinks its radius to r_2 , extends its membrane towards the other pole for $\delta\phi$, then expands again. The cell will translate further through the fluid during the first leg than during the third, thereby producing a net translation after a complete cycle. Quantify this.

Solution. Parametrize the sphere S by (ϕ, θ) , where ϕ is the azimuthal coordinate. Let $u_T(\phi)$ be the tangential deformation field in the direction of the meridians. We need the following information from hydrodynamics: For a sphere of radius a , the stress vector corresponding to a rigid translation \hat{U} is constant in the same direction of \hat{U} at every point of the sphere (this

property seems to hold uniquely for the sphere). Its value, incidentally, is $3\mu\hat{U}/2a$.

Exercise 19.10 The corresponding total force is $\hat{F} = 6\pi\mu a\hat{U}$, the famous Stokes drag for the sphere.

Exercise 19.11 Show that the countervelocity associated with the deformation field u^T is simply the average over the sphere surface

$$\bar{U} = -\frac{1}{4\pi a^2} \int_S u_T \sin\phi \, dS. \quad (98)$$

Continuing There is no translation associated with expansion and contraction legs of the swimming stroke, so we need only calculate the translation associated with the first and third legs of the stroke. Suppose that the boundary vector fields during these legs are

$$u_T = \pm c \frac{\partial}{\partial\phi}.$$

On each of the first and third legs the membrane shrinks/expands by $r_i\delta\phi$. Note that the durations in time are different:

$$\Delta t_i = \delta\phi r_i / c.$$

The countervelocities, in the direction of the z -axis, are in absolute value

$$\frac{1}{4\pi a^2} \int_S c \sin\phi \, dS = \frac{c\pi}{4}.$$

Therefore, the distance traveled on each leg i is in absolute value

$$\frac{c\pi}{4} \frac{\delta\phi r_i}{c} = \frac{\pi\delta\phi r_i}{4},$$

so the distance traveled by the organism per stroke is

$$\frac{\pi\delta\phi}{4} (r_2 - r_1).$$

If the cell swims at a rate of f strokes per second, then the velocity is

$$\frac{\pi\delta\phi f}{4} (r_2 - r_1). \quad (99)$$

20 Swimming = Holonomy

A time periodic swimming stroke is given by a loop in shape space with $s(0) = s(T)$. The swimmer can make progress because the horizontal distribution is *nonholonomic*²⁸. After a complete swimming stroke, the swimmer assumes its original shape but its position in the fluid has changed by a rigid motion which is an element of the Euclidean group:

$$q(T) = g(T) \cdot q(0). \quad (100)$$

The quantity $g(T)$, which represents the net rotation and translation due to the swimming stroke, is called the *holonomy* of the connection.

In terms of the Stokes connection form, $g(t)$ satisfies the differential equation

$$g^{-1}(t) \cdot g'(t) = -A_{q(t)}(q'(t)). \quad (101)$$

Exercise 20.1 Prove this formula.

Hint. Here $q(t)$ is an arbitrary curve of located shapes with $\pi q(t) = s(t)$. There is a unique curve $g(t)$ in G such that $g(t)q(t)$ is the horizontal lift of $s(t)$. This means that

$$A\left(\frac{d}{dt}g(t)q(t)\right) = 0.$$

Use the equivariance property of the connection to finish the proof. ■

The solution to this differential equation is written *formally* as a *path ordered integral* [20]

$$g = \text{Path exp} \left(- \int_0^T A_{q(t)}(q'(t)) dt \right). \quad (102)$$

Note that the path ordering is necessary because the group of Euclidean motions is not Abelian.

²⁸From the viewpoint of control theory, one would like the horizontal distributions to be as far from integrable (in the Frobenius sense) as possible (otherwise the organism would be constrained to a submanifold of its environment!)

Proposition 20.1 If a swimming stroke is given as

$$\Sigma(t) = \Sigma + \sum_j a_j(t) \bar{v}_j, \quad 0 \leq t \leq T, \quad (103)$$

where Σ is a base shape, $\{\bar{v}_j\}$ is a basis for the vector fields along Σ , and a_j the associated amplitude functions, then after one stroke the net translation and rotation are given by

$$g = I + \sum_{m < n} \mathcal{F}_{mn} \int_0^T a_m(t) \dot{a}_n(t) dt + O(|a|^3). \quad (104)$$

Here \mathcal{F} is the curvature of the connection:

$$\mathcal{F}_{mn} = A([\bar{v}_n^h, \bar{v}_m^h]), \quad (105)$$

where $[\cdot, \cdot]$ is the Lie bracket of vector fields.

Remark 20.2 (i) The term $\sum_{m < n} \mathcal{F}_{mn} \int_0^T a_m(t) \dot{a}_n(t) dt$ (which is quadratic in the amplitude) is the first term in the expansion for the path-ordered integral (102). (ii) In most cases of interest, symmetry of the wave patterns implies that the motions of the cell are along a fixed axis. In this case the motion is independent of path in the sense that the trajectory can be broken into infinitesimal pieces rearranged and reassembled into the same trajectory. If, for example, the motion involves a rotation around one axis and a translation along another, time averaging may give erroneous results. To see where the problem occurs, consider the infinitesimal motion consisting of a rotation about the z -axis and a translation along the x -axis; the net infinitesimal motion then depends on the order in which these are taken. When reconstructing the finite motion from infinitesimal ones, this "path ordering" must be taken into account.

21 Nonspherical Self-Reparametrizing Cells

The difficulty in computing the swimming velocities for an *arbitrary deformation* of a shape is that solutions to the Stokes equations must be developed with boundary conditions prescribed on that complicated shape. It is possible, in principle, to carry out this program for cells whose average shape is geometrically simple (prolate spheroidal, for example), and even

for the general ellipsoid, but the extremely complicated analysis limits the usefulness of that method.

Calculations by Kurt Ehlers (not published before) will be presented for the following restricted situation:

The physical shape Σ will be constant, but its parametrization $q(t)$ will be time dependent. For simplicity we will write $\Sigma(t)$ for $q(t)(S^2)$; One would like to determine the importance of the particular shape, but with the same "size" (volume or surface area) on the swimming performance.

From Exercise 19.8, if we restrict to *tangential* wave forms (those thought to be responsible for the motions of *Synechococcus*), then the only solutions to the Stokes equations are those necessary to compute the stress tensor for *streaming* flow past the shape. This is a very significant simplification, since the solutions for streaming flow past objects of various geometries have been computed [9].

We present approximate formulae for the propulsive velocity of a *spheroidal cell* that swims using travelling surface waves. We show that a prolate spheroid swims faster along its axis of symmetry than a sphere or oblate spheroid of the same "size" (volume or surface area). We also derive a formula for the swimming velocity of an oblate spheroid that swims in a direction perpendicular to its axis of symmetry.

21.1 Prolate and Oblate Spheroids

In our analysis we will use the solution, due to Happel-Brenner [9], of Stokes equations with boundary conditions on a nearly spherical cell given by (here θ is the azimuthal coordinate)

$$r(\phi, \theta) = a(1 + \epsilon f(\phi, \theta)). \quad (106)$$

The Stokes extension is given as a power series in the nondimensional parameter ϵ .

Consider an ellipsoidal cell whose shape is defined by the equation

$$\frac{x^2 + y^2}{a^2} + \frac{z^2}{a^2(1 - \epsilon)^2} = 1. \quad (107)$$

If $\epsilon > 0$, then the spheroid is oblate; if $\epsilon < 0$, the spheroid is prolate. To first order in ϵ the cell's shape has polar coordinate (P_0 and P_2 are Legendre polynomials)

$$r(\theta) = a(1 - \epsilon \cos^2 \theta) = a \left(1 - \epsilon \left(\frac{1}{3} P_0(\cos \theta) + \frac{2}{3} P_2(\cos \theta) \right) \right). \quad (108)$$

Now consider travelling waves on the outer membrane of the cell of the form

$$\theta \rightarrow \theta + \eta \sin(n\theta - \omega t). \quad (109)$$

These can be envisioned as trains of waves of contractions and expansions travelling down the cell body. The main result of our analysis is as follows.

Proposition 21.1 *The swimming velocity of an oblate/prolate spheroid with major and minor axis a and $a - \epsilon$ is*

$$U = \frac{\pi}{8} \eta^2 n \omega a \left(1 - \frac{1}{2} \epsilon \right) + O(\epsilon^2, \eta^4). \quad (110)$$

Here η is the amplitude of the wave, n is the wave number, and ω is the frequency.

By normalizing the volume of the cell and amplitude of the oscillation, we show that to first order in ϵ , a prolate spheroid swims faster than an oblate spheroid by a factor of nearly 2ϵ .

21.2 Outline of the Calculation

Let (r, ϕ, θ) be spherical coordinates where θ is the azimuthal coordinate. Consider a spheroidal cell described by the coordinate

$$r = a \left(1 + \epsilon \sum_{k=0}^{\infty} f_k(\phi, \theta) \right), \quad (111)$$

where the $f_k(\phi, \theta)$'s are spherical harmonic functions that are $O(1)$ with respect to the dimensionless parameter ϵ . In the special case of axial symmetry about the z -axis, r is independent of the coordinate ϕ .

In view of Exercise 19.8, in order to find the counterflow, we need (i) the total force associated to a tangential boundary condition \vec{U} on the

spheroid, and (ii) the Stokes drag corresponding to a rigid translation \vec{t} of the spheroid.

Since the stress tensor is divergence free, instead of integrating over the spheroidal surface (111) with $\epsilon \neq 0$, we integrate over the sphere corresponding to $\epsilon = 0$ (Exercise 18.3). However²⁹ we need to find the corresponding "virtual" velocities \vec{U} and \vec{t} at the sphere.

We use a Taylor expansion to determine an approximation (to arbitrary order in ϵ) to the velocity field on the sphere leading to the original velocity field when its Stokes extension is restricted to the spheroid:

$$\mathbf{v} = \sum_{i=0}^{\infty} \epsilon^i \mathbf{v}^{(i)}, \quad p = \sum_{i=0}^{\infty} \epsilon^i p^{(i)}. \quad (112)$$

Substituting these into the Stokes equations and equating terms of like power, one finds that for each i

$$\nabla^2 \mathbf{v}^{(i)} = \frac{1}{\mu} \nabla p^{(i)}, \quad \nabla \cdot \mathbf{v}^{(i)} = 0. \quad (113)$$

The boundary conditions take the form $\mathbf{v}^{(i)} = 0$ at ∞ , and

$$\sum_{i=0}^{\infty} \epsilon^i \mathbf{v}^{(i)} = \vec{U} \quad (114)$$

on the deformed spheroid.

Exercise 21.1 Use the implicit function theorem to obtain a recursive formula for the boundary condition on the sphere,

$$\mathbf{v}^{(0)} = \vec{U}, \quad (115)$$

and

$$\mathbf{v}^{(i)} = - \sum_{j=1}^i \frac{1}{j!} a^j f^j(\phi, \theta) \left(\frac{\partial^j \mathbf{v}^{(i-j)}}{\partial r^j} \right), \quad (116)$$

and setting $r = a$.

It is possible to solve these boundary value problems on the sphere.

²⁹There is no free lunch.

This is the crux of the calculation³⁰. For the reader's benefit, and to give an idea of the algebraic complexity, we give Lamb's general solution of the Stokes equations in terms of solid spherical harmonics [15].

Proposition 21.2

$$\mathbf{v} = \sum_{m \leq -1} \nabla \phi_m + \sum_{n \leq -2} \nabla \times (\vec{r} \xi_n) + \frac{1}{\mu} \sum_{n \leq -2} \left[\frac{r^2}{2(2n+1)} \nabla p_n + \frac{n}{(n+1)(2n+1)(2n+3)} r^{2n+3} \nabla \left(\frac{p_n}{r^{2n+1}} \right) \right]. \quad (117)$$

Exercise 21.2

- (i) Show that p_{-2} and ξ_{-2} give rise to the rigid translations and rotations of the sphere;
- (ii) Show all the other terms yield no net force or torque on any shape;
- (iii) Show that only ϕ_{-1} produces a change of volume.

Remark 21.3 We checked the code by computing the force, F_z , required to rigidly push the cell in the z direction with velocity \vec{U} . We obtained

$$F_z = 6\pi\mu\hat{U}a \left(1 - \frac{1}{5}\epsilon + O(\epsilon^2) \right), \quad (118)$$

which is in agreement with [9]³¹.

21.3 Results for Prolate and Oblate Spheroids

Recall that our ellipsoidal cell is defined by the equation

$$\frac{x^2 + y^2}{a^2} + \frac{z^2}{a^2(1-\epsilon)^2} = 1. \quad (119)$$

³⁰Computer algebra is of great help. We can provide the details by e-mail to the interested reader.

³¹It is interesting to note that this linear approximation for the Stokes drag is never farther than 6% in error from the exact solutions as computed by Payne and Pell. This is true even in the extreme cases of the rod ($\epsilon = -1$) and the disk ($\epsilon = 1$) [9].

If $\epsilon > 0$ then the spheroid is oblate, if $\epsilon < 0$ the spheroid is prolate. To first order in ϵ the cell shape has polar coordinates

$$r(\theta) = a[1 - \epsilon \cos^2 \theta] = a \left[1 - \epsilon \left(\frac{1}{3} P_0(\cos \theta) + \frac{2}{3} P_2(\cos \theta) \right) \right] \quad (120)$$

Consider travelling waves on the outer membrane of the cell,

$$\theta \rightarrow \theta + \eta \sin(n\theta - \omega t). \quad (121)$$

These can be envisioned as trains of waves of contractions and expansions travelling down the cell body.

Proposition 21.3 *To second order, the propulsive velocity is*

$$U = \frac{\pi}{8} \eta^2 n \omega a \left(1 - \frac{1}{2} \epsilon \right) + O(\epsilon^2, \eta^4). \quad (122)$$

Letting $\epsilon = 0$ in (122), we recover the result for a sphere of radius a [5].

This method is not limited to problems with axial symmetry such as that considered above. This is significant since many microorganisms are not axially symmetric in shape. As an example, consider a spheroid whose axis of symmetry is the z -axis that swims along the x -axis³². The cell is described by the equation

$$\frac{x^2 + y^2}{a^2} + \frac{z^2}{a^2(1 - \epsilon)^2} = 1. \quad (123)$$

The drag is

$$F_x = 6\pi\mu\hat{U}a \left(1 - \frac{2}{5}\epsilon + O(\epsilon^2) \right). \quad (124)$$

Proposition 21.4 *If the travelling wave is now described by*

$$\phi \rightarrow \phi + \eta \sin(n\phi - \omega t), \quad (125)$$

then the velocity of propulsion is

$$U = \frac{\pi}{8} \eta^2 n \omega a \left(1 - \frac{3}{32} \epsilon \right) + O(\epsilon^2, \eta^4). \quad (126)$$

³²Some microorganisms are disk-like and swim edgewise.

21.4 Comparisons of Swimming Velocities

It is interesting to compare the swimming velocities of prolate spheroids, spheres, and oblate spheroids of the same size. Equal volume and equal surface area are equivalent conditions when calculating to first order, so we will normalize all three spheroids so that their volumes and surface areas are $\frac{4}{3}\pi a^3$ and $4\pi a^2$, respectively. The sphere, prolate spheroid, and the oblate spheroid have equatorial radii a , $a(1-\frac{1}{3}d)$, and $a(1+\frac{1}{3}d)$, respectively, where $d = |\epsilon|$ in (119). We have also normalized³³ the amplitude of oscillation so that the amplitude of oscillation at the equator for all three spheroids is $a\eta$. Other physiological constraints on the size and elastic properties of the membrane may be appropriate when applying the theory to a specific organism. The normalized velocities are:

$$U_{oblate} = \frac{\pi}{8}\eta^2 n\omega a \left(1 - \frac{20}{24}\epsilon\right),$$

$$U_{sphere} = \frac{\pi}{8}\eta^2 n\omega a,$$

$$U_{prolate} = \frac{\pi}{8}\eta^2 n\omega a \left(1 + \frac{20}{24}\epsilon\right).$$

To first order, prolate spheroid swims by a factor of nearly ϵ faster than a sphere and nearly twice that compared to an oblate spheroid.

The cyanobacterium *Synechococcus* is thought to swim using a tangential mechanism as described by (121). These organisms are $2\mu m$ long and $1\mu m$ in diameter. Observed swimming velocities are on the order of $25m\mu m/sec$. Reasonable parameters for such an organism are

$$n = 30, \eta = .02\mu m, \omega = 800s^{-1}.$$

If $\epsilon = .2$, then the prolate spheroid swims nearly $5\mu m/sec$ faster than the sphere, and $10\mu m/sec$ faster than the oblate spheroid of the equivalent sizes.

³³Velocities for other choices of normalizations are easily approximated using (122).

22 Final Remarks

The linear correction to Stokes law for prolate and oblate spheroids is amazingly accurate. It would be interesting to compute the swimming velocity of a prolate spheroid using prolate spheroidal harmonics to compare the velocity with those predicted by our model. The Stokes function for streamlines of flow has been computed by Sampson [9] and the stress tensor can be calculated.

Keller and Wu [10] presented an alternative method for investigating the effect of shape on swimming performance at low Reynolds number. The method assumes a constant vector field on a "porous" prolate spheroid shell surrounding the cell. A form for the velocity field was chosen such that the solutions to the Stokes equations could be easily obtained and such that the resulting flow agreed quantitatively with observations of actual swimming microorganisms (*paramecia*). A general porous cell model could be made by using the technique for asymmetrical cells together with this approach. It is possible that more complicated shapes and/or more complicated flows could be treated in this way. Because the flow in this approach is steady it may be possible to compute higher order terms as well.

References

- [1] Berg, H. C., *Random Walks in Biology*, expanded edition, Princeton University Press, Princeton, NJ (1993).
- [2] Blake, J. R., *A spherical envelope approach to ciliary propulsion*, *J. Fluid Mech.* **46**, 199-208 (1971).
- [3] Blake, J. R., *Infinite models for ciliary propulsion*, *J. Fluid Mech.* **49**, 209-222 (1971).
- [4] Blake, J. R., *Self propulsion due to oscillations on the surface of a cylinder at low Reynolds number*, *Bull. Austral. Math. Soc.* **3**, 255-264 (1971).
- [5] Childress, S., *Mechanics of Swimming and Flying*, Cambridge University Press, Cambridge, UK (1981).
- [6] Dusenbery, D. B., *Life at Small Scale*, Scientific American Library (1996).

- [7] Ehlers, K. M., *The geometry of swimming and pumping at low Reynolds Number*, Ph.D. Thesis, University of California, Santa Cruz (1995).
- [8] Ehlers, K. M., Samuel, A., Berg, H., Montgomery, R., *Do cyanobacteria swim using traveling surface waves?*, Proc. Nat. Acad. Sci., **93** 8340–8343 (1996).
- [9] Happel, J., Brenner, H., *Low Reynolds Number Hydrodynamics*, Prentice-Hall, Englewood Cliffs, NJ (1965).
- [10] Keller, S., Wu, T., *A porous prolate-spheroidal model for ciliated microorganisms*, J. Fluid Mech. **80:2**, 259–278 (1977).
- [11] Koiller, J., Montgomery, R., Ehlers, K., *Problems and progress in Microswimming*, J. Nonlinear Science **6**, 507–541 (1996).
- [12] Koiller, J., Raupp, M. A., Fernandez, J. D., Ehlers, K., Montgomery, R., *Spectral methods for Stokes flows*, Comput. Appl. Math., **17:3**, 343–371 (1998).
- [13] Koiller, J., Fernandez, J. D., *Efficiencies of nonholonomic locomotion problems*, Rep. Math. Phys., **42:1/2**, 165–183 (1998).
- [14] Koiller, J., Ehlers, K., Cherman, A., Delgado, J., Montgomery, R., Duda, F., *Low Reynolds number swimming in two dimensions*, in Proc. HAMSYS98, Ernesto Lacomba, J. Llibre, eds. World Scientific, River Edge, NJ, to appear.
- [15] Lamb, H. *Hydrodynamics*. Cambridge University Press, Cambridge, UK (1895).
- [16] Lighthill, M. J., *On the squirming motion of nearly spherical deformable bodies through liquids at very small Reynolds number*, Commun. Pure Appl. Math. **5**, 109–118 (1952).
- [17] Ludwig, W., *Zur theorie der flimmerbewegung (dynamik, nutzeffekt, energiebilanz)*, Z. vergl. Physiol. **13**, 397–504 (1930).
- [18] Montgomery, R., *Nonholonomic control and gauge theory*, in Z. Li, J. F. Canny, eds., *Nonholonomic motion planning*, Kluwer, Norwell, MA (1993), pp.343–377.
- [19] Purcell, E. M., *Life at low Reynolds number*. Amer. J. Phys. **45**, 3–11 (1977).
- [20] Shapere, A., Wilczek, F., *Geometry of self-propulsion at low Reynolds number*. J. Fluid Mech. **198**, 557–585 (1989).
- [21] Taylor, G. I., *Analysis of the swimming of microscopic organisms*, Proc. Roy. Soc. Lond. Ser. A **209**, 447–461 (1951).